

Research Article

OENMOP: Loss-Aware 4×4 and 5×5 and Scalable Nonblocking Optical Switches Designed for Odd–Even Routing Algorithm for Chip-Scale Interconnection Networks

Negin Bagheri Renani , Elham Yaghoubi , and Mina Mohammadirad 

Faculty of Computer Engineering, Najafabad Branch, Islamic Azad University, Najafabad, Iran

Correspondence should be addressed to Elham Yaghoubi; e.yaghoubi@pco.iaun.ac.ir

Received 22 July 2024; Revised 29 August 2025; Accepted 3 September 2025

Academic Editor: Nihal F. F. Areed

Copyright © 2025 Negin Bagheri Renani et al. Journal of Electrical and Computer Engineering published by John Wiley & Sons Ltd. This is an open access article under the terms of the Creative Commons Attribution License, which permits use, distribution and reproduction in any medium, provided the original work is properly cited.

In this paper, optical routers play an indispensable role in the ONoCs. The 4×4 , 5×5 , and scalable optical routers based on Mach–Zehnder interferometer (MZI) and microring resonator (MRR) are proposed. These routers are designed for a deadlock-free Odd–Even turning model. The four- and five-port and scalable optical routers are extended to improve network performance and physical-layer parameters for a broad range of silicon nanophotonic multicore interconnection topologies. Compared with previously reported router designs, these router designs allow quantifying improved system performance parameters in terms of insertion loss (IL) for well-known photonic interconnection topologies. Simulation results demonstrate that four- and five-port optical routers utilizing Odd–Even MRR technology significantly enhance network performance over conventional router architectures. In particular, within mesh topologies, these routers achieve remarkable reductions in IL, improving by approximately 30.22% and 68.40% compared with standard designs. The routing performance of this router is simulated by the successful transmission of a 20-Gbps optical signal at the wavelength of 1552 nm for each qualified port from a choice of physical paths. Moreover, the growth of the number of MRR used in the structure of Odd–Even scalable router design per N I/O ports has been significantly reduced compared to previous scalable MRR-based designs.

Keywords: microring resonator (MRR); Odd–Even turn model routing; optical switching; scalable optical router

1. Introduction

Optical networks-on-chip (ONoCs) have emerged as an innovative type of network-on-chip (NoC) for multiprocessor systems-on-chip. While traditional NoCs rely on electrical communication for data transmission, ONoCs utilize optical communication as an efficient alternative, offering significant advantages in networking and data transfer [1–9].

Various topologies are employed in ONoCs, including Mesh and Torus. Among these, the Mesh topology is particularly popular due to its straightforward and organized structure, making it well suited for designing two-dimensional (2D) layouts on silicon chips. In 2D Mesh networks, each routing node features four primary ports

(North, South, East, and West) for internode connectivity, along with a local port for communication with computing elements [10].

A critical component in ONoCs is the optical router, which facilitates the selection of paths between input and output ports. These routers are composed of interconnected optical switches arranged in specific topological patterns. Commonly used optical switches include microring resonators (MRRs) and Mach–Zehnder interferometers (MZIs).

To address these limitations, various MZI-based switch designs have been proposed. MZI switches exhibit superior thermal stability and a wider bandwidth in comparison to their MRR counterparts [6, 11, 12].

Furthermore, the design of a deadlock-free ONoC is crucial. Several deadlock-free turn-model algorithms have

been developed to optimize network routing [13]. Among these, the Odd–Even turn model has demonstrated the ability to provide more routing path options compared to other models [14]. Integrating targeted NoC algorithms into optical router designs removes path constraints, which in turn decreases the number of switching components needed in the router architecture. This reduction directly lowers insertion loss (IL), thereby enhancing the overall performance of Photonic Networks-on-Chip (PNoCs).

This paper introduces four-port, five-port, and scalable optical routers designed using a combination of the Odd–Even turn model routing, MRRs, and MZIs. This approach leverages the benefits of both techniques while enhancing applicability for various use cases. The evaluation results demonstrate that the proposed optical routers based on the Odd–Even turn model exhibit superior performance compared with previous designs. Improvements are observed in critical metrics such as the number of switching elements, waveguide crossings, power budget, and IL, highlighting their effectiveness for optical network applications.

The rest of the paper is organized as follows:

Section 2 explains ONoC topology and also Odd–Even turning model. In Section 4, the results of the simulation are evaluated and compared with the results from the previous routers. Section 5 presents the conclusions.

2. ONoC Topology and Odd–Even Turning Model

Topology plays a fundamental role in the design of PNoCs as it directly influences router architecture and significantly impacts overall network performance. The Odd–Even turn model ensures deadlock freedom by eliminating certain turns while maintaining path diversity and adaptability.

2.1. ONoCs Topologies. The selection of interconnection network topology is a critical aspect, as it affects both physical-layer parameters and network performance metrics. Various researchers have proposed topologies tailored to specific applications or application domains. For instance, Shacham et al. [15] introduced the first topology for photonic chip multiprocessor (CMP) networks, known as the photonic torus. This topology offers high path diversity, enabling multiple path alternatives for photonic signals. However, its access points, acting as gateways, allow each processor core to send or receive optical signals mapped to all network nodes. This design increases the likelihood of blocking within the network, leading to potential performance degradation. To address these challenges, Wang et al. [16] proposed the Nonblocking Torus topology. In this design, only two access points are assigned to each row and column of the torus network nodes. This adjustment improves latency, power consumption, and the photonic signal-to-noise ratio (SNR). Nevertheless, the photonic torus still outperforms the Nonblocking Torus in terms of IL, scalability, and total network bandwidth [16]. To minimize IL further, Chan proposed the TorusNX topology [7]. This design separates the access points into distinct units, with

modulators handling transmission and detector banks managing the reception of photonic signals. Additionally, TorusNX minimizes waveguide crossings compared with both the photonic torus and the Nonblocking Torus. This topology supports dimension-ordered routing for internal signal routing.

The 2D mesh topology, widely adopted in electrical NoCs, has also been implemented in photonic networks due to its simplicity and regular structure [17]. Despite these advantages, the photonic mesh suffers from limited path diversity, which may lead to congestion and underutilization.

This research evaluates the Mesh, TorusNX, and Nonblocking Torus topologies in order to compare the IL performance of the proposed Odd–Even MRR-based routers with other optical routers built using MRR technology.

2.2. Odd–Even Turning Model. Networks with routing capabilities are susceptible to deadlock issues [18]. Deadlock arises when two packets are in a waiting state for one another until routing decisions are made. In such situations, both packets occupy certain resources and await the release of the resources they need from each other. Consequently, the packets cannot reach their destination due to the blockage of some intermediary resources. Various routing algorithms, such as XY, west-first, north-last, negative-first, and odd–even, are employed to mitigate deadlock [19]. A practical approach to address this challenge involves applying certain rules that restrict the routing algorithms to prevent deadlock from occurring. In these routing algorithms, which operate based on turning models, specific directions are excluded. By removing certain turns while preserving route diversity, deadlock can be avoided. With these restrictions in place, the Odd–Even turn model ensures deadlock freedom, provided that 180° turns are prohibited [20].

Figure 1 illustrates the architecture of the Odd–Even. By implementing this restriction approach, the final turn model routing effectively eliminates the risk of deadlock [14]. A major benefit of the Odd–Even, compared with others, is its ability to offer a greater number and variety of possible routes by placing fewer restrictions on each node. In addition to preventing deadlock, this approach improves overall routing efficiency in the network [21, 22].

2.3. ONoC Architecture. The design of modern photonic networks is inherently complex, as their performance is highly dependent on the characteristics of the physical layer. A modification in the properties of a single photonic component can significantly influence the performance and overall architecture of the entire system, distinguishing it from traditional CMOS designs.

Figure 2 illustrates the architecture of a CMP, which comprises three functional layers: the processing cores are located in the lowest layer, known as the processing plane. This plane also serves as the source and destination for data communication. Optical interconnections between processors are established in the photonic data plane. Meanwhile, the configuration and routing functions are executed within the electronic control layer.

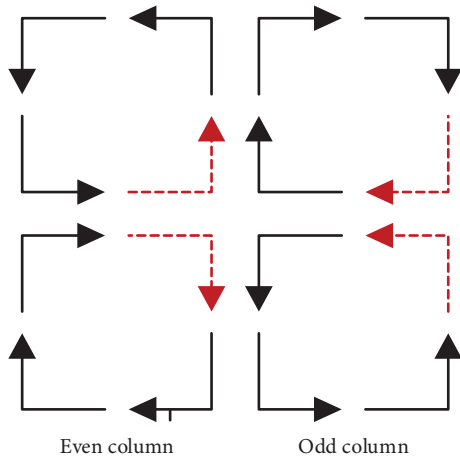


FIGURE 1: Odd-Even turn model.

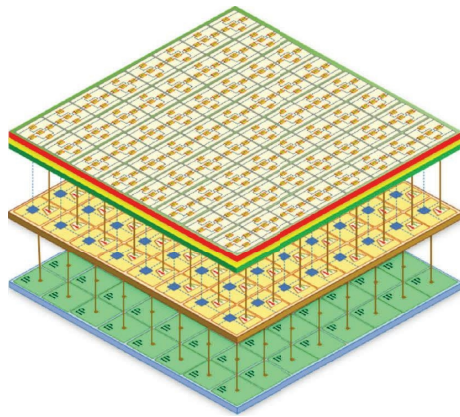


FIGURE 2: Illustration of the architecture of CMP with three functional layers [5].

The electronic control layer plays a vital role, as the photonic layer does not support logical processing. Situated at the central level of the CMP, this electronic layer enables the exchange of control signals through metal wire interconnections, illustrated as blue dashed lines. Communication between the electronic and photonic layers is facilitated via the modulation and detection (M/D) interface, depicted by brown lines, whereas router operations are coordinated through dedicated control links. The electronic network is responsible for managing message exchanges among processor cores and for controlling the switching infrastructure. In parallel, the optical communication network facilitates high-efficiency routing of light packets across the chip, achieving low latency and optimized efficiency. Optical routers, structured as $n \times n$ arrays of optical switches, establish connections between local I/O ports. Notably, an optical router requires activation only once to set up an optical circuit, thus eliminating the need for continuous switching during high-bit-rate optical data transmission. Additionally, the use of wavelength-division multiplexing (WDM) technology facilitates ultrahigh-bandwidth optical communication.

3. Proposed Odd-Even Optical Routers

In this section, we present 4×4 , 5×5 , and $N \times N$ optical routers which are designed for Odd-Even turn model routing by using MRR and MZI switches. Additionally, by reducing the number of constraints imposed on each node, the Odd-Even routing algorithm expands the variety of possible paths and significantly improves network routing performance by effectively preventing deadlocks. In the following, we will discuss three designs of optical routers.

3.1. MZI-Based Odd-Even Four-Port Optical Router. The schematic of the first proposed design is presented in Figure 3. The MZI has been used as the switching element to send optical data in the network in this design. The designs shown in Figure 3 were used to route the nodes of the network of the even and odd columns, respectively. Overall, the proposed router has been designed using four MZIs as a 4×4 matrix with four inputs (i.e., N_i , E_i , S_i , and W_i) and four outputs (i.e., N_o , E_o , S_o , and W_o), respectively, for the north, east, south, and west ports. Moreover, the switching elements have been from M1 to M4.

Tables 1 and 2 present the routing of network nodes of the even and odd columns, respectively. Overall, each four-port router can cover 16 routes. Moreover, sending data from the input port of one port to the output port of the same port, as U-Turn is not allowed in PNoC. Additionally, in the routing tables of even column (Table 1) and odd column (Table 2), data transfer from East to North and from East to South and also North to West and South to West are limited, sequentially. Thus, any four-port Odd-Even router can pass optical data through 10 possible routes. In each place of the routing tables, MZIs are specified must be in Cross state.

3.2. MZI-Based Odd-Even Five-Port Optical Router. The schematic of the first proposed design is illustrated in Figure 4. In this design, the MZI has been used as the switching element to send optical data in the network. The structures shown in Figure 4 are used to route the nodes of the network of the odd and even columns, respectively. Overall, the proposed routes have been designed using six MZIs as 5×5 with four inputs (i.e., N_i , E_i , S_i , W_i , and C_i) and four outputs (i.e., N_o , E_o , S_o , W_o and C_o), respectively, for North, East, South, West, and the ports connected to IP-Core. Moreover, the switching elements have been from M1 to M6.

Tables 3 and 4 present the routing of network nodes of the even and odd columns, sequentially. In general, each five-port router can cover 25 routes. Based on mentioned points, the U-Turn data transmission routes specified in the table diameter are not allowed. Thus, any five-port Odd-Even router can pass optical signals through 18 possible routes. In each house of the routing tables of Mach-Zehnder switches, data transfer direction from the specified input port to the specified output port must be in Cross state.

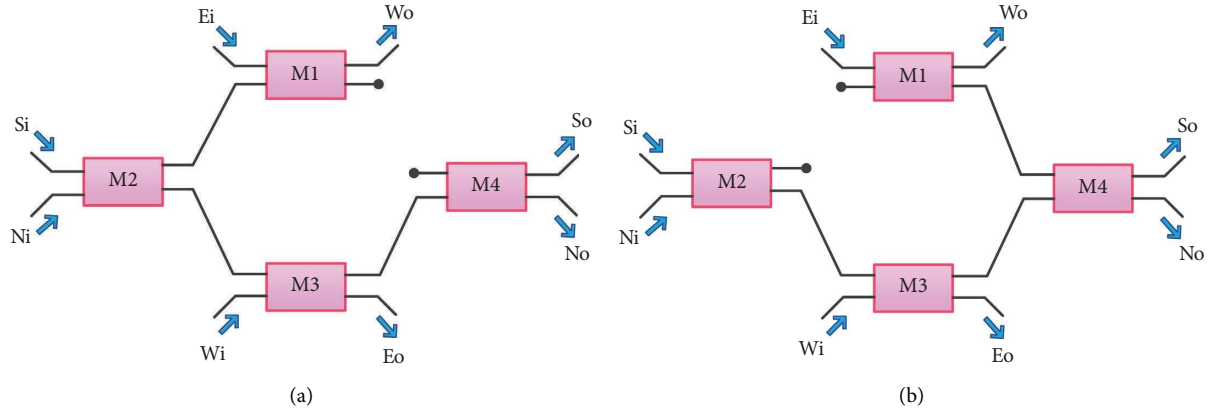


FIGURE 3: MZI-based Odd-Even four-port optical router. (a) Even column and (b) odd column node routers.

TABLE 1: Even column of Odd-Even four-port router based on MZI.

| Output | Input | | | |
|--------|-------------------|-------------------|-------------------|-------------------|
| | Ni | Ei | Si | Wi |
| No | No U-Turn allowed | X | M2, M3, M4 | M3, M4 |
| Eo | M2, M3 | No U-Turn allowed | M2, M3 | M3 |
| So | M2, M3, M4 | X | No U-turn allowed | M3, M4 |
| Wo | M2, M1 | M1, M4 | M2, M1 | No U-turn allowed |

TABLE 2: Odd column of Odd-Even four-port router based on MZI.

| Output | Input | | | |
|--------|-------------------|-------------------|-------------------|-------------------|
| | Ni | Ei | Si | Wi |
| No | No U-turn allowed | M1 | M2, M3, M4 | M3, M4 |
| Eo | M2, M3 | No U-turn allowed | M2, M3 | M3 |
| So | M2, M3, M4 | M1, M4 | No U-turn allowed | M3, M4 |
| Wo | X | M1, M4 | X | No U-turn allowed |

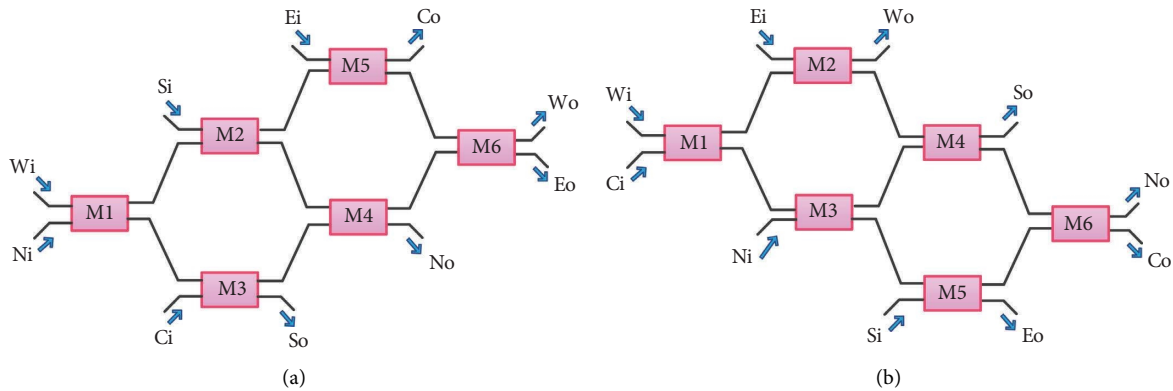


FIGURE 4: MZI-based Odd-Even five-port optical router. (a) Even column and (b) odd column node routers.

3.3. MZI-Based Odd-Even Scalable Optical Router. The schematic of the third proposed design can be seen in Figure 5. This design is developed from the Odd-Even five-

port router designs proposed in the previous section to N-ports optical routers by maintaining properties of the Odd-Even algorithm as scalable for use in PNoC.

TABLE 3: Even column of Odd–Even five-port router based on MZI.

| Output | Input | | | | |
|--------|-------------------|-------------------|-------------------|-------------------|-------------------|
| | Ni | Ei | Si | Wi | Ci |
| No | No U-Turn allowed | X | M2, M4 | M1, M3, M4 | M2, M4 |
| Eo | M1, M3, M4, M6 | No U-Turn allowed | M2, M4, M6 | M1, M2, M5, M6 | M3, M4, M6 |
| So | M1, M3 | X | No U-Turn allowed | M1, M3 | M3 |
| Wo | M1, M3, M4, M6 | M5, M6 | M2, M4, M6 | No U-Turn allowed | M3, M4, M6 |
| Co | M1, M2, M5 | M5 | M2, M5 | M1, M2, M5 | No U-turn allowed |

TABLE 4: Odd column of Odd–Even five-port router based on MZI.

| Output | Input | | | | |
|--------|-------------------|-------------------|-------------------|-------------------|-------------------|
| | Ni | Ei | Si | Wi | Ci |
| No | No U-Turn allowed | M2, M4, M6 | M5, M6 | M1, M2, M4, M6 | M1, M3, M5, M6 |
| Eo | M3, M5 | No U-Turn allowed | M5 | M1, M3, M5 | M1, M3, M5 |
| So | M3, M4 | M2, M4 | No U-Turn allowed | M1, M2, M4 | M1, M3, M4 |
| Wo | X | M2 | X | No U-Turn allowed | M1, M2 |
| Co | M3, M4, M6 | M2, M4, M6 | M5, M6 | M1, M2, M4, M6 | No U-Turn allowed |

Given the significance of the number of optical devices used in optical routers per N input and output ports and as the core of this design is the same five-port router based on MZI, the number of MZI switches used in the proposed router structure can be calculated using (1).

As can be seen, the five-port router consists of 6 MZI and 14 waveguide bending. Also, the proposed scalable structure allows the development of inputs from one side and outputs

from the other to N ports according to equation (1) while maintaining the limitations of the Odd–Even turn model routing. Additionally, the design of this structure includes 0 waveguide crossings according to equation (2) and the number of waveguide bending of the structure can be calculated according to equation (3).

$$\begin{aligned} \text{IF } N \geq 5 \text{ then } N_{\text{MZI}} &= 6 + 2(N - 5) = 2N - 4 = 2(N - 2) \\ \longrightarrow N_{\text{MZI}} &= 2(N - 2), \end{aligned} \quad (1)$$

$$\begin{aligned} \text{IF } N < 5 | N = 4 \text{ then } N_{\text{MZI}} &= 6 + 2(N - 5) \\ &= 2N - 4 = 2(N - 2) \longrightarrow N_{\text{MZI}} = 2(N - 2) = 4, \end{aligned}$$

$$\begin{aligned} \text{IF } N \geq 5 \ N_{\text{WGC}} &= 0, \\ \text{IF } N < 5 \ N_{\text{WGC}} &= 0, \end{aligned} \quad (2)$$

$$\begin{aligned} \text{IF } N \geq 5 \text{ then } N_{\text{Bend}} &= 14 + 4(N - 5) = 4N - 6 \\ \longrightarrow N_{\text{Bend}} &= 4N - 6. \end{aligned} \quad (3)$$

3.4. MRR-Based Odd–Even Four-Port Optical Router. The schematic of the fourth proposed routers is designed in Figure 6. In these designs, MRR switches have been utilized as a switching element in order to send optical data to the network. Figure 6(a) is used to route the network nodes of odd columns and Figure 6(b) even columns. The proposed 4×4 optical routers which are designed for Odd–Even turn model routing include four MRRs. These routers have four inputs (i.e., Ni, Ei, Si, and Wi) and four outputs (i.e., No, Eo, So, and Wo) for North, East, South, and West ports, respectively. The MRRs are named from R1 to R4.

Tables 5 and 6 present the routing of network nodes of odd and even columns, respectively. Generally, each four-port router can cover 16 routes, of which U-Turn data routes are not allowed. In addition to the U-Turn routes, according

to the operation of the Odd–Even algorithm, in the routing table of odd column routers, data transfer is not allowed from North to West and South to West. Meanwhile, in the routing table of even column routers, data transfer is not allowed from East to North and from East to South. Thus, any four-port Odd–Even router can pass optical data through 10 possible routes. In each place of the routing tables, MRRs are identified as switching elements that must be ON to be able to transmit data from the input port to the output port by deflecting light.

3.5. MRR-Based Odd–Even Five-Port Optical Router. The schematic of the fifth proposed design is seen in Figure 7. MRRs play a decisive role in this design as a switching

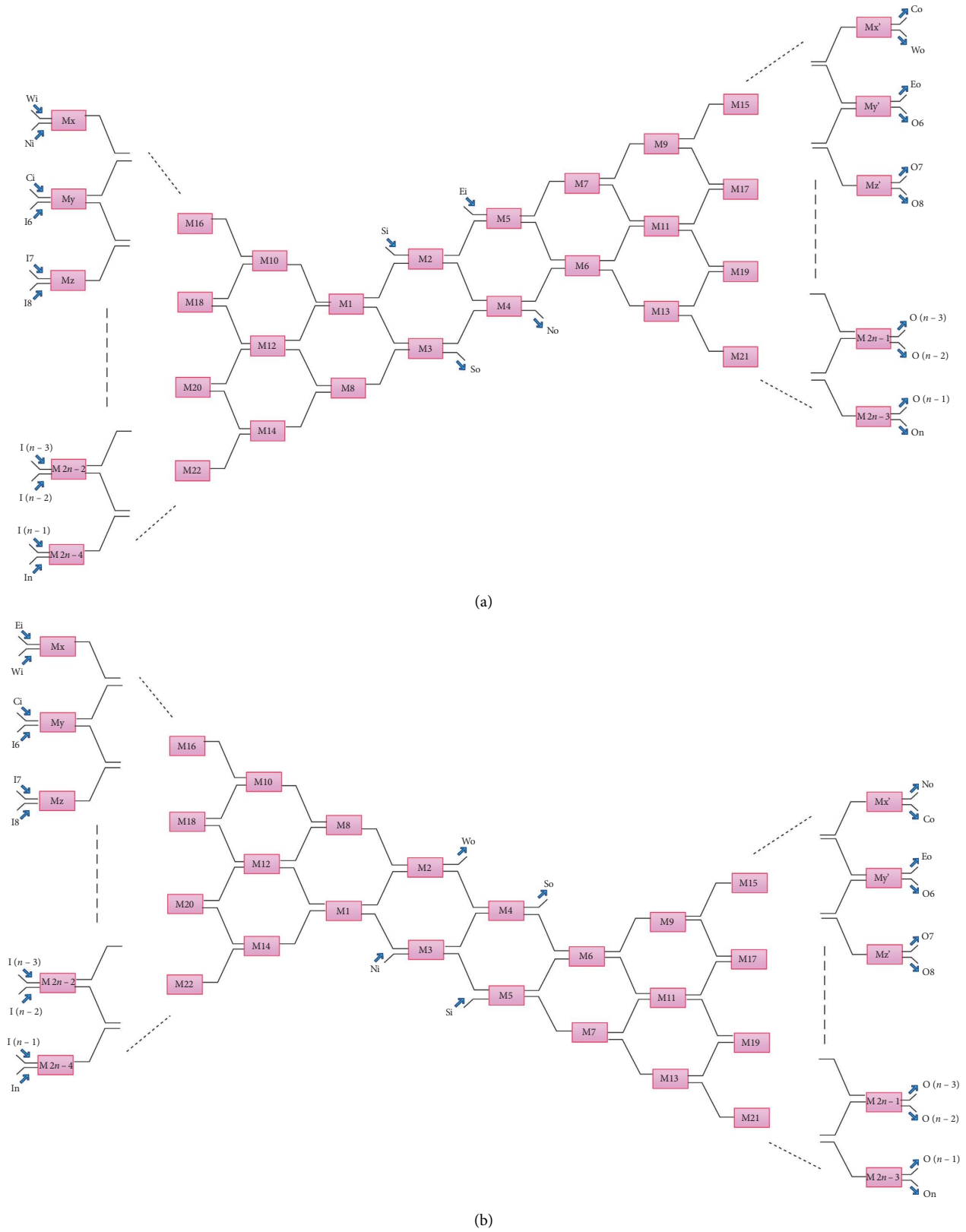


FIGURE 5: Odd-Even scalable optical router based on MZI. (a) Odd column and (b) even column node routers.

element to send optical data to the network. The designs presented in Figure 7 are used to route the network nodes of odd and even columns, respectively. Overall, the provided

5×5 optical routers, designed for the Odd-Even turn model, have six MRRs. The routers include five inputs (i.e., Ni, Ei, Si, Wi, and Ci) and five outputs (i.e., No, Eo, So, Wo, and Co)

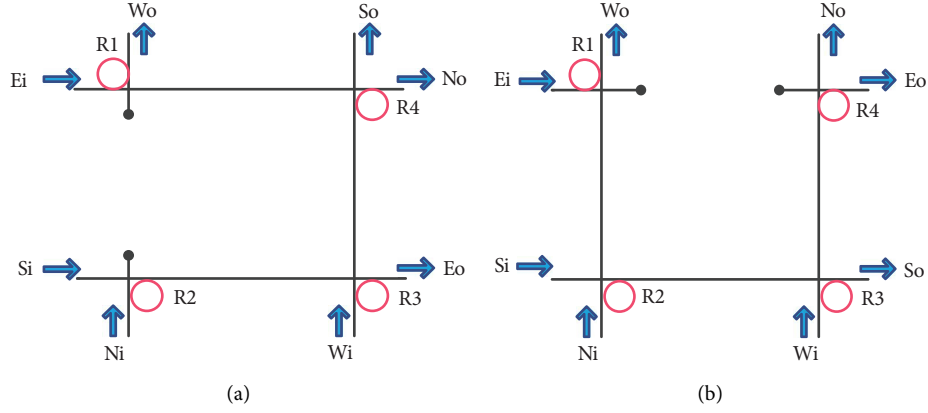


FIGURE 6: Odd-Even four-port optical router based on MRR. (a) Odd column and (b) even column node routers.

TABLE 5: Routing of four-port Odd-Even optical router's odd column based on MRR.

| Item | Input | Output | PSE |
|------|-------|--------|--------|
| 1 | N | E | R2 |
| 2 | N | S | R2, R3 |
| 3 | S | E | — |
| 4 | S | N | R3, R4 |
| 5 | W | N | R4 |
| 6 | W | S | — |
| 7 | W | E | R3 |
| 8 | E | N | — |
| 9 | E | S | R4 |
| 10 | E | W | R1 |

TABLE 6: Routing of four-port Odd-Even optical router's even column based on MRR.

| Item | Input | Output | PSE |
|------|-------|--------|------------|
| 1 | E | W | R1 |
| 2 | N | E | R2, R3, R4 |
| 3 | N | W | — |
| 4 | N | S | R2 |
| 5 | S | W | R2 |
| 6 | S | E | R3, R4 |
| 7 | S | N | R3 |
| 8 | W | N | — |
| 9 | W | S | R3 |
| 10 | W | E | R4 |

for North, East, South, and West processing core ports, respectively. In this design, the switching elements are known from R1 to R6.

Tables 7 and 8 present the routing of the network nodes of odd and even columns, respectively. Here, each 5×5 optical router can cover 25 routes, where U-Turn data routes are not allowed based on the points mentioned in the previous sections. In addition to the U-turn routes, the routing table of odd-column routers prohibits data transfer from North to West and South to West. Besides, in the routing table of even-column routers, odd data transfer from East to North and from East to South is not allowed. Therefore, each five-port Odd-Even router can pass optical

data through 18 possible routes. In each space of the routing tables, MRRs are identified as switching elements that must be set to ON to be able to transmit data from the input port to the output port by deflecting light.

3.6. MRR-Based Odd-Even Scalable Optical Router. The schematic of the sixth proposed design is depicted in Figure 8. This design is developed from the Odd-Even five-port router scheme, while maintaining the properties of the Odd-Even algorithm on a scalable base for PNoC. As already stated, given the significance of the number of optical devices used in the structure of optical routers per N input and output ports, the number of MRRs used in the proposed routing structure can be calculated using equation (4). In this design, which is an extension of the MRR-based Odd-Even five-port optical router design, 6 MRRs are in the central core of this design. Moreover, the inputs develop on the one side and outputs on the other side while maintaining the limitations imposed by the Odd-Even algorithm. Therefore, two MRRs are added to the previous design to increase one input/output port to a scalable design. Furthermore, as presented in equations (5) and (6), given the type of design, the number of waveguide bending is zero. The number of waveguide bending is equal to the number of microrings used in the router in this structure.

$$\begin{aligned} \text{IF } N \geq 5 \text{ then } N_{\text{MRR}} &= 6 + 2(N - 5) = 2N - 4 \\ &= 2(N - 2) \longrightarrow N_{\text{MRR}} = 2(N - 2), \end{aligned} \quad (4)$$

$$\begin{aligned} \text{IF } N < 5 \text{ then } N_{\text{MRR}} &= 6 + 2(N - 5) = 2N - 4 \\ &= 2(N - 2) \longrightarrow N_{\text{MRR}} = 2(N - 2) = 4, \end{aligned}$$

$$\text{IF } N \geq 5 \text{ and } N < 5 \text{ } N_{\text{Bend}} = N_{\text{MRR}}, \quad (5)$$

$$\text{IF } N \geq 5 \text{ and } N < 5 \text{ } N_{\text{WGC}} = N_{\text{MRR}}. \quad (6)$$

All the proposed 4×4 , 5×5 , and $N \times N$ Odd-Even optical routers are presented in various designs incorporating both mentioned optical switches, enabling their use in diverse applications and leveraging the advantages of both optical elements.

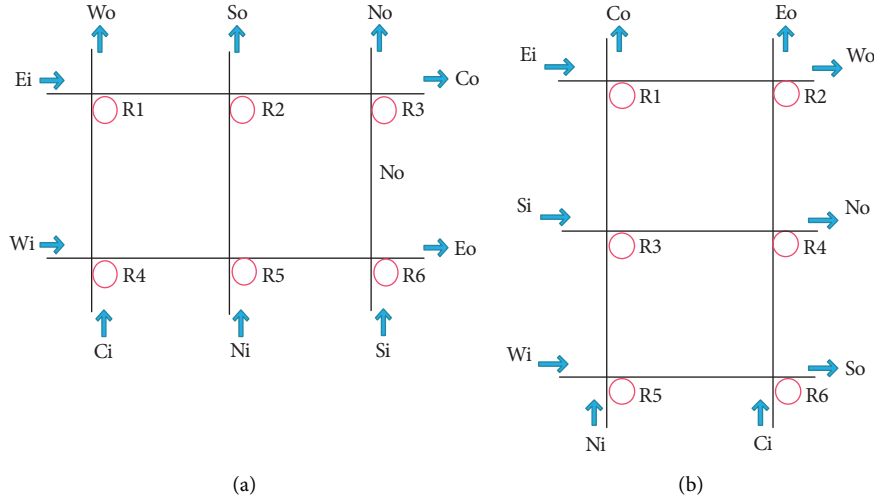


FIGURE 7: Odd-Even five-port optical router based on MRR (a) Odd column and (b) even column node routers.

TABLE 7: Routing of Odd-Even five-port router's odd column based on MRR.

| Item | Input | Output | PSE |
|------|-------|--------|--------|
| 1 | N | E | R5 |
| 2 | N | S | — |
| 3 | N | C | R2 |
| 4 | S | E | R6 |
| 5 | S | N | — |
| 6 | S | C | R3 |
| 7 | W | N | R6 |
| 8 | W | S | R5 |
| 9 | W | E | — |
| 10 | W | C | R6, R3 |
| 11 | E | N | R3 |
| 12 | E | S | R2 |
| 13 | E | W | R1 |
| 14 | E | C | — |
| 15 | C | E | R4 |
| 16 | C | N | R1, R3 |
| 17 | C | S | R4, R5 |
| 18 | C | W | — |

TABLE 8: Routing of Odd-Even five-port router's even column based on MRR.

| Item | Input | Output | PSE |
|------|-------|--------|--------|
| 1 | N | E | R5, R6 |
| 2 | N | W | R1 |
| 3 | N | S | R5 |
| 4 | N | C | — |
| 5 | S | W | R4, R2 |
| 6 | S | E | R4 |
| 7 | S | N | — |
| 8 | S | C | R3 |
| 9 | W | N | R6, R4 |
| 10 | W | S | — |
| 11 | W | E | R6 |
| 12 | W | C | R5 |
| 13 | E | W | — |
| 14 | E | C | R1 |
| 15 | C | E | — |
| 16 | C | N | R4 |
| 17 | C | W | R2 |
| 18 | C | S | R6 |

4. Experimental Analysis

To simulate our proposed 4×4 , 55 , and $N \times N$ MZI-based optical routers, designed for the Odd-Even turn model routing, we utilize an OptiSystem Version 17 simulator to evaluate the proposed optical routers from the aspects of IL, Q-factor, minimum bit error ratio, and eye diagram.

OptiSystem is a powerful and widely used simulation tool for designing and analyzing optical communication systems. It is particularly well suited for simulating complex optical networks, including both analog and digital components. The reasons for using OptiSystem include its ability to model a wide range of optical devices and systems, including fiber optics, modulation techniques, and signal processing. It offers a user-friendly interface and a comprehensive set of features, allowing for accurate system performance analysis. Additionally, OptiSystem supports

both time-domain and frequency-domain simulations, making it a versatile choice for optimizing system parameters, predicting performance, and ensuring the reliability of optical communication networks.

Moreover, due to the potential advantages and applications of the OptiSystem simulation, as well as its comprehensive features and optical elements required for simulating the proposed routers, this simulator has been utilized.

In addition, we use the proposed MZI switch in [23] as a switching element for optical routers design. The size of the switch is about $93 \times 1.7 \mu\text{m}^2$. Table 9 outlines the parameters configured for the simulation of the proposed routers. The subsequent sections will present and analyze the results obtained from simulating these routers.

An externally modulated laser source was employed in this study, driven by a 20-Gbps pseudorandom bit sequence

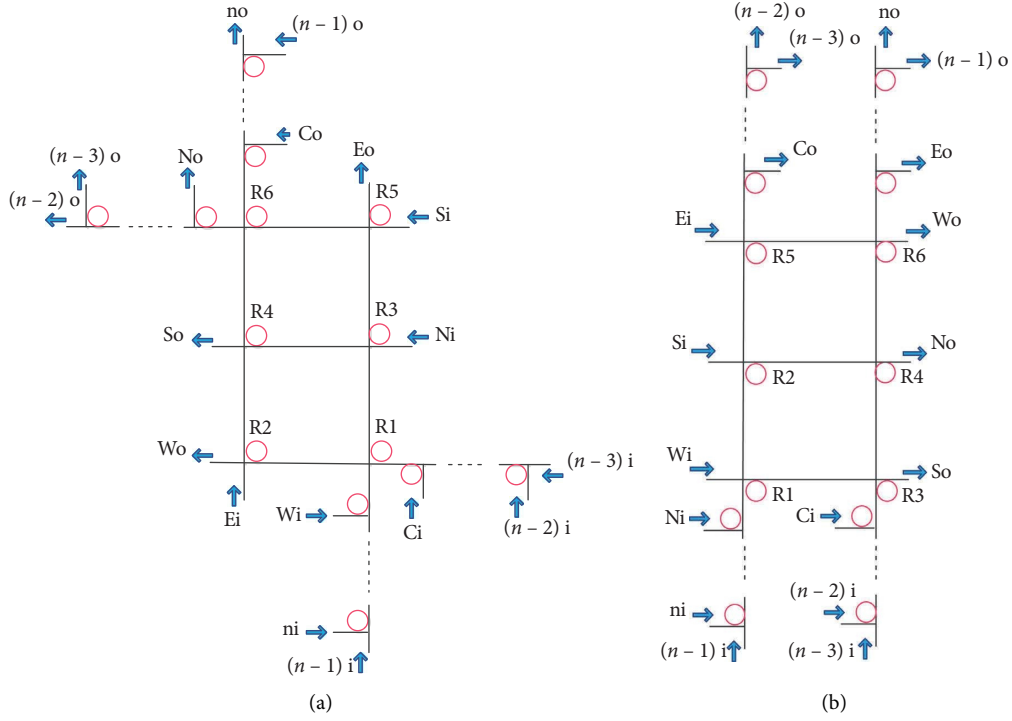
FIGURE 8: Odd-Even $N \times N$ scalable optical router based on MRR: (a) odd column and (b) even column node routers.

TABLE 9: Interconnect configuration parameters in OptiSystem.

| Simulation parameter | Value |
|------------------------|-------------------------------|
| Bandwidth | 20 Gb/s |
| Wavelength | 1552 nm |
| Size of the MZI switch | $93 \times 1.7 \mu\text{m}^2$ |
| Power | 1 mw |

TABLE 10: Interconnect configuration parameters in Phoenixsim.

| Simulation parameter | Value |
|-------------------------------|----------|
| Laser power | 20 dB/m |
| Detector sensitivity index | -25 dB/m |
| Bandwidth | 2.5 Gb/s |
| Message size | 1024 bit |
| Router buffer size | 64 bit |
| Number of wavelength channels | 16 |

produced by a pulse pattern generator. At the output stage, a PIN photodetector combined with a low-pass filter was utilized. The optical signals from the output ports of the optical router were subsequently analyzed using a digital communication analyzer to examine the waveforms and eye diagrams.

We have utilized the PhoenixSim simulator written in C++ language and developed in the OMNET++ [24–26] environment platform to simulate our proposed 4×4 , 5×5 , and $N \times N$ MRR-based optical routers which is designed for the Odd-Even routing algorithm. PhoenixSim provides physical layer characterizations, such as IL. The configuration parameters for simulating the proposed MRR-based routers are presented in Table 10.

TABLE 11: Factors of insertion loss.

| Simulation parameter | Value |
|----------------------|-------------------|
| Waveguide crossing | 0.16 db [27] |
| Waveguide bending | 0.005 db/90° [28] |
| MZI-bar | 1.1 db [23] |
| MZI-cross | 1.2 db [23] |

4.1. Evaluation of the Proposed MZI-Based Optical Routers Designed for Odd-Even Routing. In the proposed optical routers, four paths are excluded as per the Odd-Even routing algorithm. This exclusion leads to a reduction in waveguide crossings and optical components, thus enhancing physical layer metrics such as IL. Additionally, the reduction in waveguide crossings and switching components contributes to a decrease in area consumption. Another key benefit of these optical routers is their assurance of deadlock-free operation, all while maintaining minimal system complexity. A key parameter examined in this study is IL. To evaluate the IL, the values provided in Table 11 are used, referencing data from published sources.

In an ONoC, the bandwidth, Q-factor, laser power, and message size are interrelated parameters that influence the performance, efficiency, and reliability of data communication. Here is a detailed explanation of their relationships.

1. Bandwidth and Q-factor

- Bandwidth represents the range of frequencies over which an optical channel can effectively transmit signals. Higher bandwidth allows for faster data rates and higher throughput.

- Q-Factor is a measure of signal quality, derived from the eye diagram, reflecting noise levels, signal distortion, and intersymbol interference (ISI).

Relationship:

- Trade-Off: increasing bandwidth often introduces higher dispersion and ISI, which can degrade the Q-factor. This happens because wider frequency components can suffer from chromatic dispersion or bandwidth limitations of components (e.g., modulators and detectors).
- Optimized bandwidth usage: for a fixed optical system, there is an optimal bandwidth where the Q-factor is maximized. Beyond this range, noise and distortion may dominate, leading to higher bit error rates (BERs).

2. Laser power and Q-factor

- Laser power is the optical power generated by the laser source. It affects the signal strength and is crucial for overcoming losses in optical interconnects.
- Q-factor depends on SNR. Higher laser power generally improves the SNR, leading to a better Q-factor. However, excessive laser power can introduce nonlinear effects (e.g., self-phase modulation or thermal effects), degrading signal quality.

Relationship:

- Low power: insufficient laser power leads to signal attenuation, reducing the Q-factor and increasing BER.
- Optimal power: properly tuned laser power ensures a high Q-factor by balancing SNR and minimizing nonlinear distortions.

3. Message size and bandwidth

- Message size refers to the volume of data transmitted in a single communication session. Larger message sizes require more time or higher bandwidth for transmission.
- Bandwidth is the channel capacity available for transmitting data.

Relationship:

- Larger messages: for a fixed bandwidth, transmitting larger messages takes more time, increasing latency.
- High bandwidth requirement: larger message sizes may require higher bandwidth to maintain low latency and meet performance demands.

4. Message size and Q-factor

- Larger messages involve prolonged transmission, increasing the likelihood of accumulated noise, distortion, and ISI over time.
- Q-factor degradation: as message size increases, maintaining a high Q-factor becomes challenging, especially if the bandwidth and laser power are not optimized.

5. Combined interplay

- Bandwidth, laser power, and message size affect Q-factor:
 - To transmit larger messages quickly, higher bandwidth is needed, but this can degrade the Q-factor due to dispersion and noise.
 - Increasing laser power can improve the Q-factor for large messages, but excessive power introduces nonlinearities.
 - The optimal combination of these parameters ensures reliable, high-speed communication with acceptable BER.

Summary

In an ONoC:

- Higher bandwidth enables faster data transfer but can degrade the Q-factor if not properly optimized.
- Laser power must be balanced to ensure sufficient signal strength while avoiding nonlinear effects that harm the Q-factor.
- Larger message sizes demand more bandwidth and laser power but can lead to cumulative signal degradation, affecting the Q-factor.

Effective design of ONoC systems involves finding the optimal trade-off among these parameters to achieve high data rates, low latency, and reliable communication.

4.1.1. Physical Layer Analysis of MZI Four-Port Router Using Odd-Even. IL, describing the attenuation of lightwave signal power during transmission, plays a pivotal role in performance assessment. Ensuring its minimization in the design phase contributes to reliable signal delivery and facilitates network expansion with enhanced bandwidth utilization. IL can be determined by measuring the decrease in optical signal power as it passes through the network.

The functionality of the optical router is simulated using the OptiSystem simulator, with eye diagrams employed for analysis. A 20-Gbps non-return-to-zero optical signal at a wavelength of 1552 nm is used. This optical signal traverses the 10 proposed four-port optical routers, utilizing the Odd-Even free-deadlock algorithm to achieve optimal Q-factor (quality factor) and minimum BER performance criteria. The Q-factor, which directly indicates the performance and reliability of digital communications, is used to assess signal quality, while the BER serves as the ultimate measure of quality in optical interconnections [6].

Q-factor and minimum BER are determined from the measured transmission spectra, as shown in Table 12 for both the odd and even columns of the Odd-Even MZI-based four-port optical routers. This table also illustrates the IL in each input/output path of the optical switching device.

The outcomes of the simulations for the photonic router reveal that, in the least favorable scenario, the highest BER is 2.37612e-012, and the lowest Q-factor value is 6.91278 for both the odd and even columns of the Four-Port Optical Router Based on Odd-Even MZI Architecture.

TABLE 12: Optical analysis results of the proposed MZI-based Odd–Even four-port optical router.

| Path | Path IL (dB) | Odd column | | Path IL (dB) | Even column | |
|---------|--------------|---------------|----------------|--------------|---------------|-----------------|
| | | Max. Q factor | Min. BER | | Max. Q factor | Min. BER |
| Ei → No | 2.4 | 6.92007 | 2.25698e – 012 | — | — | — |
| Ei → So | 2.3 | 6.91958 | 2.26478e – 012 | — | — | — |
| Ei → Wo | 1.1 | 6.92406 | 2.19435e – 012 | 1.1 | 6.92406 | 2.19435e – 012 |
| Ei → Eo | NUT | NUT | NUT | NUT | NUT | NUT |
| Ni → So | 3.4 | 6.91278 | 2.37612e – 012 | 3.4 | 6.91278 | 2.37612e – 012 |
| Ni → No | NUT | NUT | NUT | NUT | NUT | NUT |
| Ni → Wo | — | — | — | 2.4 | 6.92007 | 2.25698e – 012 |
| Ni → Eo | 2.3 | 6.91958 | 2.26478e – 012 | 2.3 | 6.91958 | 2.26478 e – 012 |
| Si → No | 3.4 | 6.91278 | 2.37612e – 012 | 3.4 | 6.91278 | 2.37612e – 012 |
| Si → so | NUT | NUT | NUT | NUT | NUT | NUT |
| Si → Wo | — | — | — | 2.3 | 6.91958 | 2.26478e – 012 |
| Si → Eo | 2.4 | 6.92007 | 2.25698e – 012 | 2.4 | 6.92007 | 2.25698e – 012 |
| Wi → No | 2.3 | 6.91958 | 2.26478e – 012 | 2.3 | 6.91958 | 2.26478e – 012 |
| Wi → So | 2.4 | 6.92007 | 2.25698e – 012 | 2.4 | 6.92007 | 2.25698e – 012 |
| Wi → Wo | NUT | NUT | NUT | NUT | NUT | NUT |
| Wi → Eo | 1.1 | 6.92406 | 2.19435e – 012 | 1.1 | 6.92406 | 2.19435e – 012 |

In the best-case scenario, the minimum BER is 2.19435e-012, and the maximum quality factor is 6.92406 for both columns. Given that the required BER within optical systems is required to remain below 10e-9 and a signal integrity factor of 6 indicates a reliable system without faults, these results confirm that the proposed MZI four-port router, employing the Odd–Even routing algorithm, is well suited for ONOCs. An optical PIN receiver coupled with a low-pass filter is positioned at the router's output port for capturing optical signals and forwarding them to a digital communication analyzer. The eye diagram for a wavelength input of 1552 nm, corresponding to the ten possible routing paths, is shown in Figure 9 for the four-port optical router designed using MZI. The eye diagrams clearly display the delivery of a 20-Gbps optical signal once it propagates across the router. Since every eye pattern remains open, it becomes evident that all four suggested ports effectively deliver the 20-Gbps data-bearing optical signal. Nonetheless, the attenuation in certain input/output connections of the router with the four proposed ports leads to the presence of noise in the eye diagrams of these particular paths.

For the Si → No path, the IL is 3.4 dB for the odd column of the Odd–Even MZI-based four-port router, which is greater than that of the remaining paths in the designed router. Consequently, the eye diagram for this path will probably demonstrate some noise, and the clarity of this diagram is not as distinct as the others (Figure 9(b)).

4.1.2. Physical Layer Parameters for Odd–Even MZI-Based Five-Port Router. The optical signal is passed through 18 proposed MZI-based five ports optical routers using the Odd–Even turn model; therefore, Q-factor and minimum BER metrics are attained. The Q-factor and minimum BER can be calculated as presented in Table 13 for both odd and even columns MZI-based five-port optical routers. The IL in each input/output path of the optical router is depicted in this table.

The simulation results show that, in the worst case, the maximum amount of BER is 2.57691e-012, and the minimum amount of the Q-factor is 6.90127 for both odd and even columns of Odd–Even MZI-based five-port router, respectively. Moreover, in the best case, the minimum amount of BER and maximum amount of Q-factor are 2.18939e-012 and 6.92438 for both odd and even columns of MZI-based five-port router. Therefore, as highlighted earlier, a BER below 10^{-9} and a Q-factor of 6 ensure a fault-free system, confirming that the proposed optical router is suitable for ONOCs using the Odd–Even routing model.

The eye diagram at an input wavelength of 1552 nm for the 18 possible routing paths is presented in Figure 10 for an MZI-based five-port optical router.

The IL in Ni → Wo is 4.6 dB for the even column of the Odd–Even MZI-based five-port optical router, exceeding the IL of the remaining paths in the proposed router. As a result, the eye pattern for this path may show some noise, and its clarity is not as distinct as the others (Figure 10(b)).

4.1.3. Examining the Results of the Proposed MZI-Based Odd–Even Scalable Router Design. The MZI-based Odd–Even scalable router design is examined in Section 3. Furthermore, the analysis of the proposed design led to the development of general formulas for calculating the MZI switches, waveguide crossings, and waveguide bends for the proposed router based on the number of input/output ports (N). The number of switching elements used in our design is the most significant factor affecting IL. Table 14 presents a comparison of the proposed design with previous MZI-based scalable designs, focusing on the number of switching elements utilized in the optical router design for each N I/O port.

As can be seen in Figure 11, as the network scales up, the number of the MZI of the proposed Odd–Even scalable optical router increases with a lower slope than the other studied routers. To be more precise, the core of the proposed

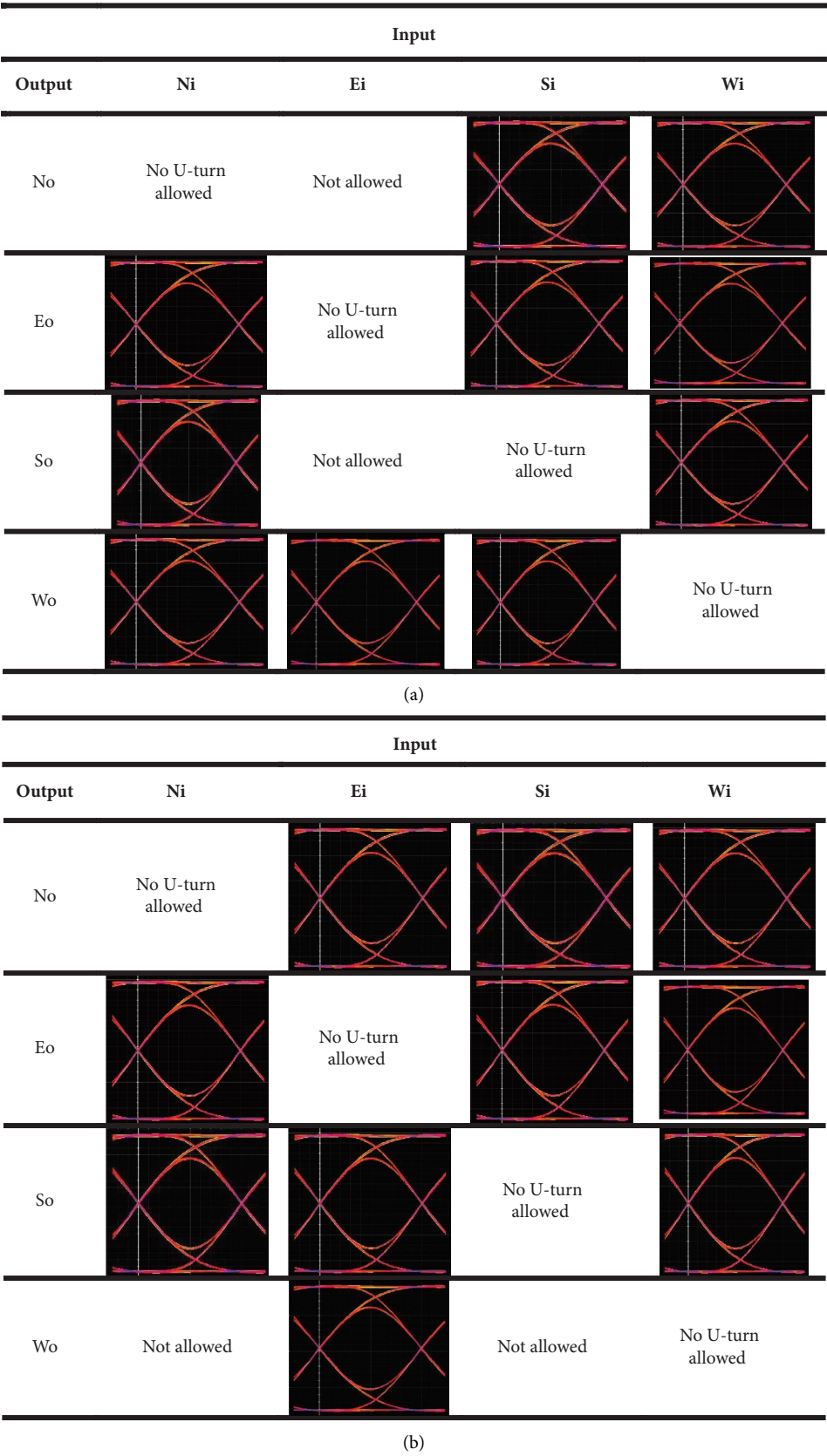


FIGURE 9: Eye diagrams for the 10 possible input–output routings through the Odd–Even four-port optical router, using 20-Gbps optical data at a wavelength of 1552 nm. (a) Odd column. (b) Even column.

TABLE 13: Optical analysis results of proposed MZI-based Odd–Even five-port optical routers.

| Path | Path IL (dB) | Odd column | | Path IL (dB) | Even column | |
|---------|--------------|---------------|----------------|--------------|---------------|-----------------|
| | | Max. Q factor | Min. BER | | Max. Q factor | Min. BER |
| Ei → No | 3.5 | 6.91201 | 2.38908e – 012 | — | — | — |
| Ei → So | 2.3 | 6.91958 | 2.26478e – 012 | — | — | — |
| Ei → Wo | 1.1 | 6.92438 | 2.18939e – 012 | 2.3 | 6.91958 | 2.26478e – 012 |
| Ei → Eo | NUT | NUT | NUT | NUT | NUT | NUT |
| Ei → Co | 3.6 | 6.91121 | 2.40261e – 012 | 1.1 | 6.92438 | 2.18939e – 012 |
| Ni → So | 2.4 | 6.91908 | 2.27291e – 012 | 2.3 | 6.91958 | 2.26478e – 012 |
| Ni → No | NUT | NUT | NUT | NUT | NUT | NUT |
| Ni → Wo | — | — | — | 4.6 | 6.90127 | 2.57691e – 012 |
| Ni → Eo | 2.3 | 6.91958 | 2.26478e – 012 | 4.5 | 6.90244 | 2.55571 e – 012 |
| Ni → Co | 3.5 | 6.91201 | 2.38908e – 012 | 3.5 | 6.91201 | 2.38908e – 012 |
| Si → No | 2.4 | 6.91908 | 2.27291e – 012 | 2.4 | 6.91908 | 2.27291e – 012 |
| Si → So | NUT | NUT | NUT | NUT | NUT | NUT |
| Si → Wo | — | — | — | 3.5 | 6.91201 | 2.38908e – 012 |
| Si → Eo | 1.1 | 6.92438 | 2.18939e – 012 | 3.4 | 6.91278 | 2.37612 e – 012 |
| Si → Co | 2.3 | 6.91958 | 2.26478e – 012 | 2.3 | 6.91958 | 2.26478e – 012 |
| Wi → No | 4.5 | 6.90244 | 2.55571e – 012 | 3.4 | 6.91278 | 2.37612e – 012 |
| Wi → So | 3.3 | 6.91352 | 2.36371e – 012 | 2.4 | 6.91908 | 2.27291e – 012 |
| Wi → Wo | NUT | NUT | NUT | NUT | NUT | NUT |
| Wi → Eo | 3.6 | 6.91121 | 2.40261e – 012 | 4.4 | 6.90357 | 2.53547e – 012 |
| Wi → Co | 4.5 | 6.90244 | 2.55571e – 012 | 3.5 | 6.91201 | 2.38908e – 012 |
| Ci → No | 4.6 | 6.90127 | 2.57691e – 012 | 2.3 | 6.91958 | 2.26478e – 012 |
| Ci → So | 3.2 | 6.91424 | 2.35182e – 012 | 1.1 | 6.92438 | 2.18939e – 012 |
| Ci → Wo | 2.4 | 6.91908 | 2.27291e – 012 | 3.6 | 6.91121 | 2.40261e – 012 |
| Ci → Eo | 3.5 | 6.91201 | 2.38908e – 012 | 3.5 | 6.91201 | 2.38908e – 012 |

Note: NUT, No U-Turn Allowed.

Abbreviation: IL, insertion loss.

design is the same as the proposed Odd–Even five-port router design with fewer optical devices. When an I/O port is added, only one optical switch is added from each side of our scalable router designed on the Odd–Even turn model. Accordingly, leading to a slight expansion of the number of optical devices in the design; therefore, the number of switching elements applied in the proposed design increases linearly, unlike the two other designs. Moreover, the proposed design is deadlock free, while the other optical routers are designed generally (Table 14). Therefore, there is a possibility of deadlock in applying these routers in PNoC. As a result, the proposed Odd–Even five-port scalable router is a suitable option for use in PNoC.

In optical communication systems, the eye opening is intricately linked to the Q-factor, which measures the signal quality and its capacity to differentiate between various levels (e.g., 1's and 0's). The eye opening, which shows how distinct the signal levels are, is the vertical distance between the eye diagram's highest and lowest points. The eye opening has a direct correlation with the Q-factor. A bigger eye opening is typically associated with a greater Q-factor.

Generally, an eye diagram with a Q-factor of 6.92406 is very distinct and easy to understand. The eye opening is typically big for Q-factor values 6.9, indicating that the signal can be easily distinguished from noise. An eye-opening value of 0.89 is generally indicated by a Q-factor of 6.92406 in best case in proposed MZI-based Odd–Even four-port optical router. In an optical communication system, the eye width is the horizontal opening of the eye diagram that shows the

time margin permitted for error-free data detection. As shown in Table 15, this value in the best case for MZI-based Odd–Even four- and five-port optical routers are equal to 0.88 and 8, respectively, indicating a high-performance system with minimal temporal distortions.

4.1.4. Compare Odd–Even MZI-Based Four- and Five-Optical Router With Other Compared Optical Routers. Initially, a comparison was made between the Odd–Even four- and five-port optical routers and previously reported routers utilizing MZIs. The comparison focused on several key metrics: the number of MZIs and waveguide crossings, the quantity of waveguide bends, maximum IL, minimum Q-factor, and maximum BER. Tables 16 and 17 present a comparative analysis of the MZI-based four- and five-port routers designed for the Odd–Even routing algorithm alongside other generic MZI-based routers reviewed in the literature.

Our proposed 4×4 and 5×5 optical routers, designed using the Odd–Even routing algorithm, feature a reduced number of switching elements and waveguide crossings compared to the aforementioned routers. This reduction in switching elements directly contributes to a decrease in device area and overall power consumption [32]. Moreover, minimizing waveguide crossings helps enhance the router's performance by reducing crosstalk and IL [33]. As a result, the proposed routers are well suited for PNoC applications. Waveguide crossings, when present, can induce additional

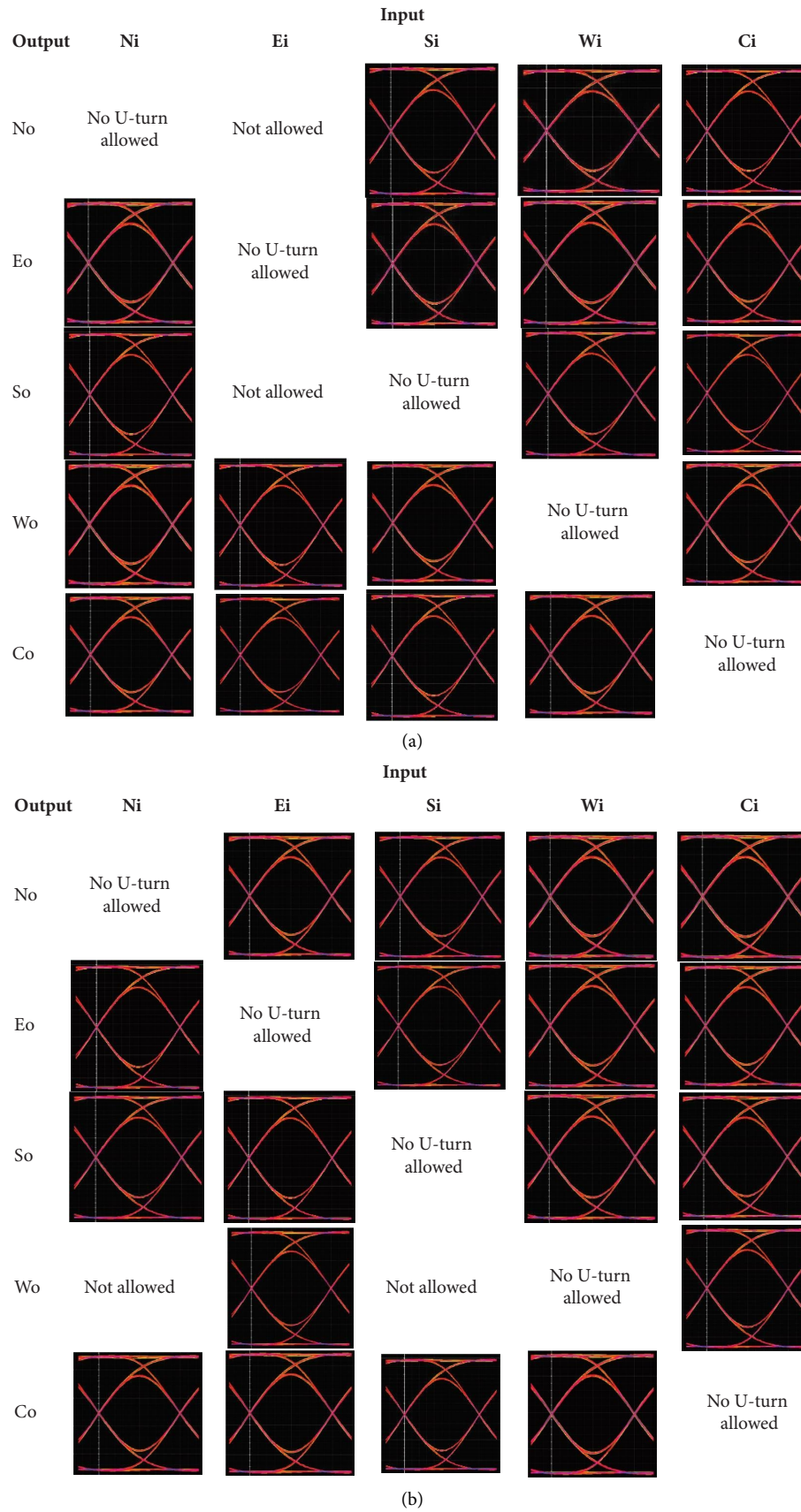


FIGURE 10: Eye diagrams for the 10 possible input-output routings through the Odd-Even five-port optical router, using 20-Gbps optical data at a wavelength of 1552 nm. (a) Odd column. (b) Even column.

TABLE 14: The number of switching elements in Odd–Even $N \times N$ scalable optical routers based on Mach–Zehnder interferometer switches.

| Optical router | The number of MZI |
|-----------------------------------|-------------------|
| Proposed Odd–Even scalable router | $2(N - 2)$ |
| Scalable router [29] | $N(N - 1)/2$ |
| Scalable router [30] | $N(N - 2)$ |

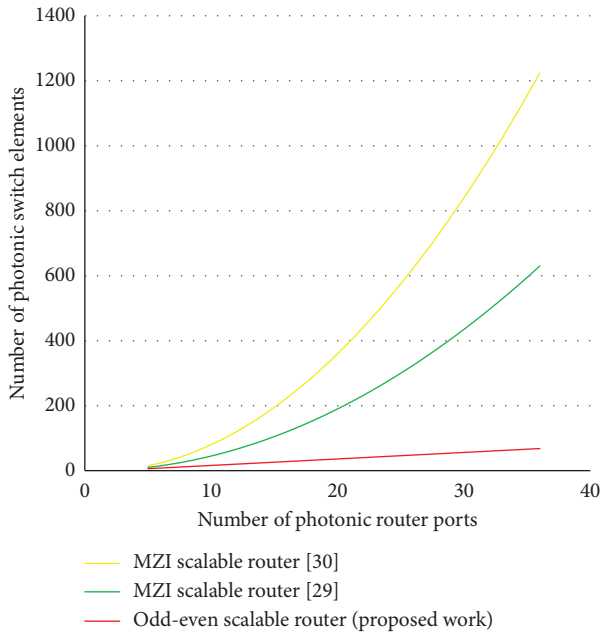


FIGURE 11: The growth of the number of MZI switches because of an increase in the number of I/O ports.

losses in the router; therefore, limiting their occurrence leads to improved performance. Furthermore, reducing the number of switching elements (such as MZIs) results in a more compact router design.

Given the variety of PNoC architectures, the need for optical routers with different input/output configurations is critical. The number of switching elements directly influences the size of the router, and for a four-port router, the use of MZI switches results in fewer switching elements and waveguide crossings compared to typical MZI-based routers. A key advantage of MZI-based routers is their ability to handle high-speed data transmission with nano-second switching times [32].

These designs, with their minimized MZI count, achieve relatively favorable performance in terms of speed and loss characteristics. The proposed routers are capable of transmitting a 20-Gbps optical data signal from each of the four or five input ports. Furthermore, they support broadband operation over multiple WDM optical signals, a capability that MRR-based switches do not offer.

When evaluating the performance of the proposed routers, the results indicate that the Odd–Even four- and five-port optical routers deliver superior network performance across various parameters, including IL, number of MZIs, waveguide crossings, minimum Q-factor, and

maximum BER, compared with previously designed routers (as shown in Tables 16 and 17).

This paper presents a design for optical routers with distinctive characteristics, including the type of switches employed and the number of MZIs. Compared with optical routers discussed in other studies, the proposed routers require less space and feature simpler designs. Additionally, these routers exhibit lower loss, and the impact of these advantages on enhancing the physical layer parameters in photonic networks is also highlighted.

4.2. Evaluation of Proposed MRR-Based Optical Routers Designed for Odd–Even Turn Model Routing

4.2.1. Compare Odd–Even MRR-Based Four- and Five-Port Optical Router With Other Compared Optical Routers. The measurement of IL is influenced by several factors, including propagation, waveguide crossings, waveguide bending, the passage through a ring or photonic switching element (PSE) in the off-state, and the drop into a ring or PSE in the on-state.

Accordingly, the designs of the four- and five-port routers, intended for the Odd–Even turn model routing, were developed with these loss-influencing parameters in mind, ensuring that the router minimizes loss in each path.

The proposed router designs stand out due to the exclusive use of 1×2 PSE switches. These routers feature the fewest MRRs in comparison to previous MRR-based four- and five-port optical routers. Our routers represent the first 4×4 , 5×5 , and scalable optical routers designed for the Odd–Even turn model, achieving the lowest number of MRRs. With fewer MRRs, the proposed routers require less space and have a simpler design compared to other optical routers documented in the literature. Additionally, these routers exhibit lower IL, and the impact of this advantage on enhancing the physical layer parameters in photonic networks will be discussed in this section.

This crucial aspect has been taken into account in the design of MRR-based four- and five-port optical routers developed for the Odd–Even turning model.

A key aspect in minimizing IL in PNoCs is employing optical routers with the fewest optical components.

Tables 18 and 19 compare the number of optical elements (MRRs), the number of waveguide crossings, and the number of waveguide bending used in the structure of our four- and five-port optical routers, which are designed for Odd–Even turn model routing, drawing on MRR designs from previous studies, respectively.

4.2.2. The Maximum IL for MRR-Based Odd–Even Four- and Five-Port Optical Routers in Different Topologies. All the routers mentioned in Tables 18 and 19 have been modeled under the same conditions, with the simulation outcomes examined to assess the performance of the proposed routers. According to the simulation results, the diagrams of Figure 12 illustrates the maximum IL as the network scales for each of the designed four-port routers listed in Table 18,

TABLE 15: Comparison table of the worst-case and best-case scenarios about the eye diagram.

| Proposed MZI routers | | Parameters | | | |
|----------------------|------------|-------------|------------|-----------|--------------------|
| | | Eye opening | Eye height | Eye width | Decision threshold |
| 4 port | Worst case | 0.88 | 4.66 | 0.8 | 0.23 |
| | Best case | 0.89 | 6.08 | 0.88 | 0.39 |
| 5 port | Worst case | 1 | 0.8 | 2.3 | 6.9 |
| | Best case | 0.9 | 0.9 | 0.8 | 6.9 |

across the Mesh, Nonblocking Torus, and TorusNX topologies.

The results are collected for all the proposed routers when used in different topologies.

As can be seen in the above diagrams, the proposed four-port Odd–Even router has better performance in PNoC by reducing the maximum IL in the photonic network for each of topologies. Based on these simulation results, the chart of Figure 13 shows maximum IL as the network increases for all the proposed five-port routers mentioned in Table 19 when used in Mesh topology.

As can be seen in the above chart, the proposed 5×5 optical router using the Odd–Even turn model has shown better performance in PNoC by reducing the maximum level of IL under mesh topology.

4.2.3. The Improvement of Maximum IL in MRR-Based Odd–Even Four-Port Optical Router. One of the key parameters that impacts the quality of optical signal transmission is the number of waveguide crossings along its path. Similarly, the amount of active MRRs traversed also contributes to overall loss. By employing the Odd–Even turn model in the proposed four-port optical router, both of these factors are significantly minimized. As indicated in Table 12, the loss associated with waveguide bending is about 0.005 dB per 900, which can be regarded as negligible. Furthermore, the design requires only four MRRs to establish full connectivity among five ports, eliminating the need for physical address remapping between inputs and outputs. Under large-scale configurations, the achieved insertion losses are 30.87 dB for Mesh, 49.50 dB for Nonblocking Torus, and 37.05 dB for TorusNX topologies. These results highlight a marked reduction in loss compared with previously introduced router structures. A detailed comparison of the maximum losses with other designs is provided in Table 20.

Following the review of the results for designing and simulating the proposed MRR-based five-port router, it was observed that the proposed optical router, unlike the two other designs [38, 39], which are the general routers in this study, can prevent dead-lock over the PNoC due to the use of Odd–Even turn model routing in this paper. Additionally, the Odd–Even deadlock-free algorithm performs better than other PNoC deadlock-free algorithms due to the greater number of candidate routes over the network [21]. Consequently, the proposed Odd–Even five-port optical router design is more advantageous than the PXY router based on the XY deadlock algorithm, as it provides a higher number of candidate routes. The reduction in the number of optical devices used in the optical router leads to a decrease in IL,

which in turn enhances the physical layer and overall network performance. This improvement was 6.53%, 43.57%, and 68.40% for the proposed Odd–Even five-port router compared with the PXY and 5×5 optical routers [38, 39], respectively.

4.2.4. Power Budget. The optical power budget is a critical factor in developing optical network architectures capable of precisely transmitting signals along a transmission path. It represents the amount of power necessary to propagate the signal through an optical link.

This parameter is vital for assessing the network's bandwidth utilization and its resilience to insertion-related power losses. Maximum optical power budget is referred to as the power threshold, denoted by P . If the optical power budget exceeds P , nonlinear effects occur, resulting in increased IL and an undesirable shift in the frequency of the MRR. Conversely, the detector sensitivity, denoted by S , represents the lower limit of the optical power budget. If the optical power budget falls below S , the receiver will be unable to detect the light. The optical power budget is defined as the difference between P and S , as expressed in the following equation [17, 40].

$$P - S \geq IL_{\max} + 10 \log_{10}^n. \quad (7)$$

Based on Equation (7), n represents the permissible count of wavelength channels, denoted by IL_{\max} , and IL_{\max} refers to the peak IL [17, 40].

To evaluate the performance of the MRR-based 4×4 router, designed for the Odd–Even turning model, within the Mesh, Nonblocking Torus, and TorusNX topologies, we set the power budget to 35 dB, as per data provided by commercial transmitter and receiver vendors such as Perle Company. With this power budget of 35 dB, the optical power budget for our proposed Odd–Even four-port router enables the mesh topology to expand to 196 nodes.

In comparison, networks utilizing the Cuiting [36], Original, StraightPath, and Symmetric routers are limited to just 64 nodes. In a 64-node mesh network, when using the Cuiting [36], Helix-h, Original, Symmetric, and StraightPath routers, the number of available wavelength channels is 1, 13, 2, 3, and 6, respectively. In contrast, our proposed Odd–Even router supports 22 wavelength channels. Additionally, in a 64-node Nonblocking Torus, when using the Helix-h, Symmetric, and StraightPath routers, only 3, 1, and 1 wavelength channels are available, respectively. In comparison, the Odd–Even router provides 6 wavelength channels.

TABLE 16: Compare the design based on MZI Odd–Even optical router with four ports.

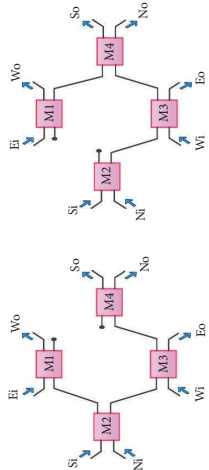
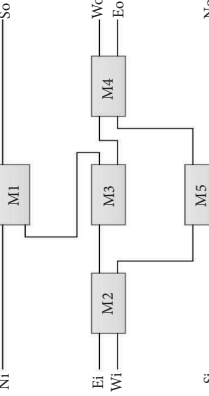
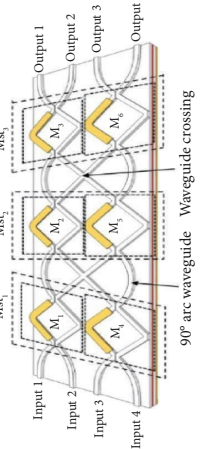
| Odd–Even four port (this work) | NLR-OP four port [6] | Four-port optical router [31] |
|---|--|---|
|  |  |  |
| Number of MZIs: 4 | Number of MZIs: 5 | Number of MZIs: 6 |
| Number of waveguide crossings: 0 | Number of waveguide crossings: 0 | Number of waveguide crossings: 2 |
| Number of waveguide bending: 6 | Number of waveguide bending: 8 | Number of waveguide bending: 8 |
| Max insertion loss: 3.4 dB | Max insertion loss: 2.65 dB | Max insertion loss: 3.6 dB |
| Max Q-factor: 6.91278 | Max Q-factor: 6.91772 | Max Q-factor: 6.91121 |
| Min BER: 2.37612e – 012 | Min BER: 2.16347e – 012 | Min BER: 2.40261e – 012 |

TABLE 17: Comparison of the design based on MZI Odd-Even optical router with five ports.

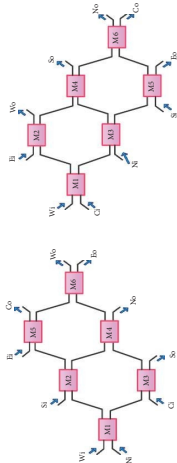
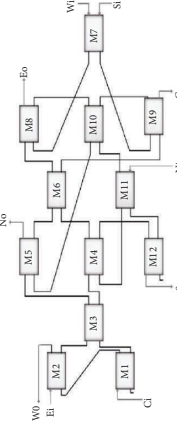
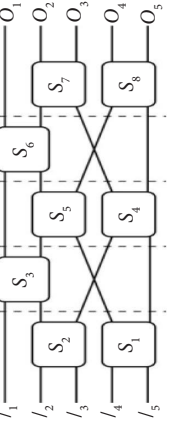
| Odd-Even five port (this work) | Five-port optical router [9] | Five-port optical router [10] |
|---|--|---|
|  |  |  |
| Number of MZIs: 6 | Number of MZIs: 12 | Number of MZIs: 8 |
| Number of waveguide crossings: 0 | Number of waveguide crossings: 6 | Number of waveguide crossings: 2 |
| Number of waveguide bending: 14 | Number of waveguide bending: 40 | Number of waveguide bending: 8 |
| Max insertion loss: 4.6 dB | Max insertion loss: 11.51 dB | Max insertion loss: 5.6 dB |
| Min Q-factor: 6.90127 | Max Q-factor: 6.92419 | Max Q-factor: 6.88669 |
| Min BER: 2.57691e-012 | Min BER: 2.19234e-012 | Min BER: 2.85511e-012 |

TABLE 18: Comparison of the Odd-Even 4×4 optical router with other with other MRR-based generic routers.

| Optical routers | Number of waveguide bending | Number of microring resonators | Number of waveguide crossings |
|--------------------------------|-----------------------------|--------------------------------|-------------------------------|
| Original [34] | 4 | 8 | 10 |
| StraightPath [35] | 8 | 8 | 12 |
| Symmetric [35] | 4 | 8 | 8 |
| Helix-h [8] | 16 | 8 | 8 |
| Four-port optical router [36] | 36 | 4 | 9 |
| RRW [3] | — | 14 | 14 |
| Odd-Even four port (this work) | 0 | 4 | 4 |

TABLE 19: Comparison of the Odd-Even 5×5 optical router with other MRR-based generic routers.

| Optical routers | Number of waveguide bending | Number of microring resonators | Number of waveguide crossings |
|--------------------------------|-----------------------------|--------------------------------|-------------------------------|
| PXY [37] | 26 | 12 | 9 |
| Hao Jia [38] | 11 | 8 | 8 |
| Zhihua [39] | 4 | 16 | 14 |
| SMOR [4] | — | 8 | 6 |
| Odd-Even five port (this work) | 0 | 6 | 6 |

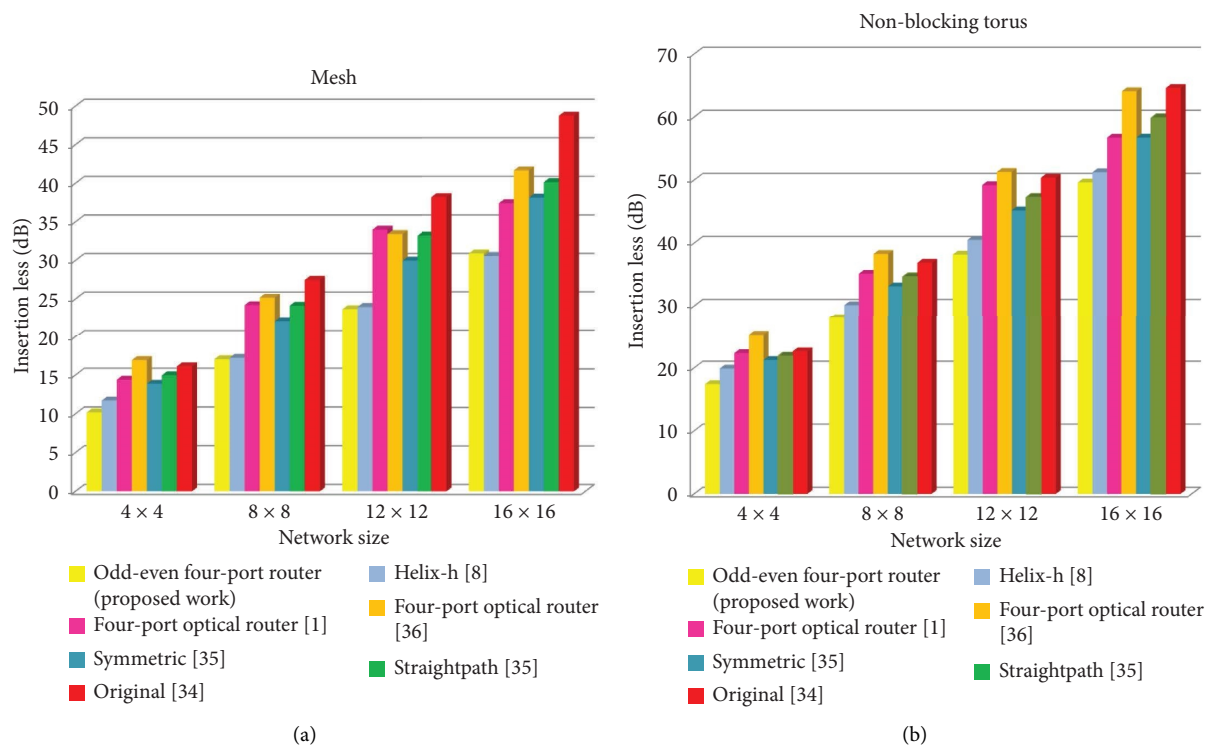


FIGURE 12: Continued.

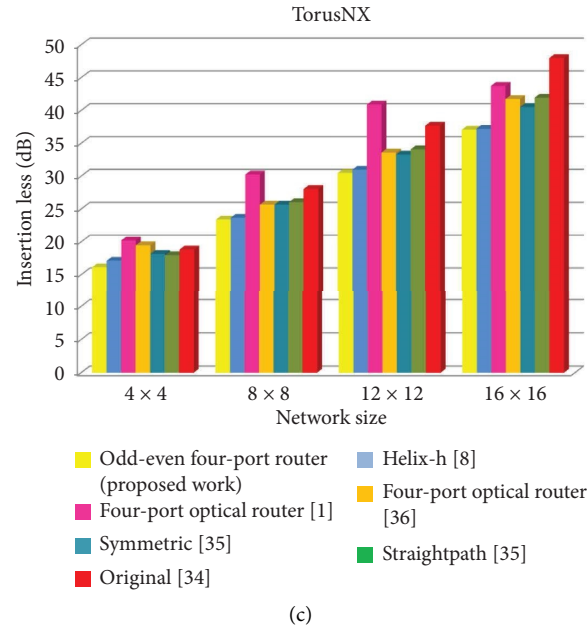


FIGURE 12: Maximum possible insertion loss breakdowns of various network sizes and different routers for (a) Mesh, (b) Nonblocking Torus, and (c) TorusNX.

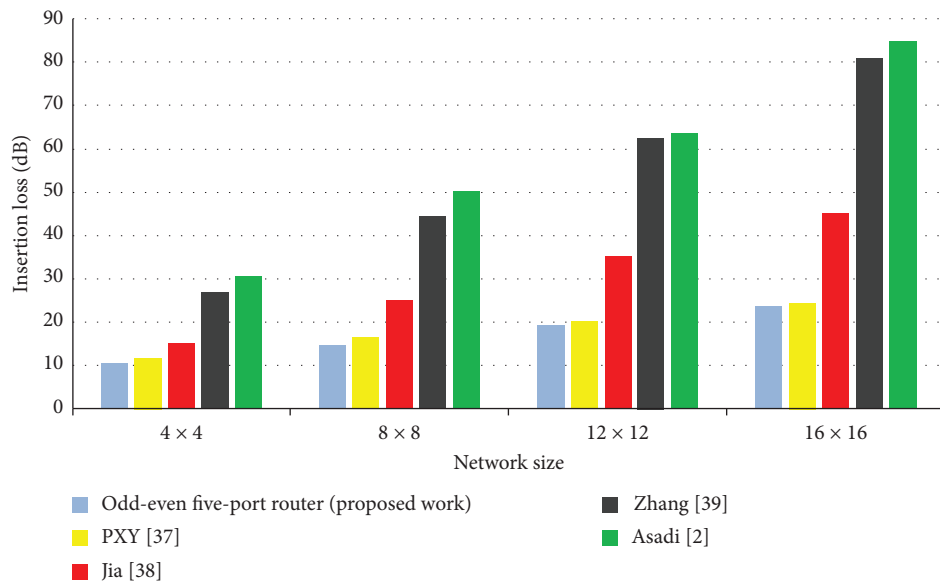


FIGURE 13: Maximum insertion loss analysis for different routers and network scales in mesh topology.

TABLE 20: Maximum insertion loss reduction in MRR-based Odd-Even four-port routers.

| Optical routers | Mesh (%) | Nonblocking Torus (%) | TorusNX (%) |
|-------------------------------|----------|-----------------------|-------------|
| Helix-h [8] | 2.04 | 4.80 | 1.28 |
| Four-port optical router [36] | 30.22 | 20.79 | 22.75 |
| Symmetric [35] | 21.45 | 13.67 | 8.54 |
| StraightPath [35] | 27.27 | 17.51 | 10.37 |
| Original [34] | 37.35 | 22.65 | 18.80 |
| Four-port optical router [1] | 25.46 | 18.39 | 29.15 |

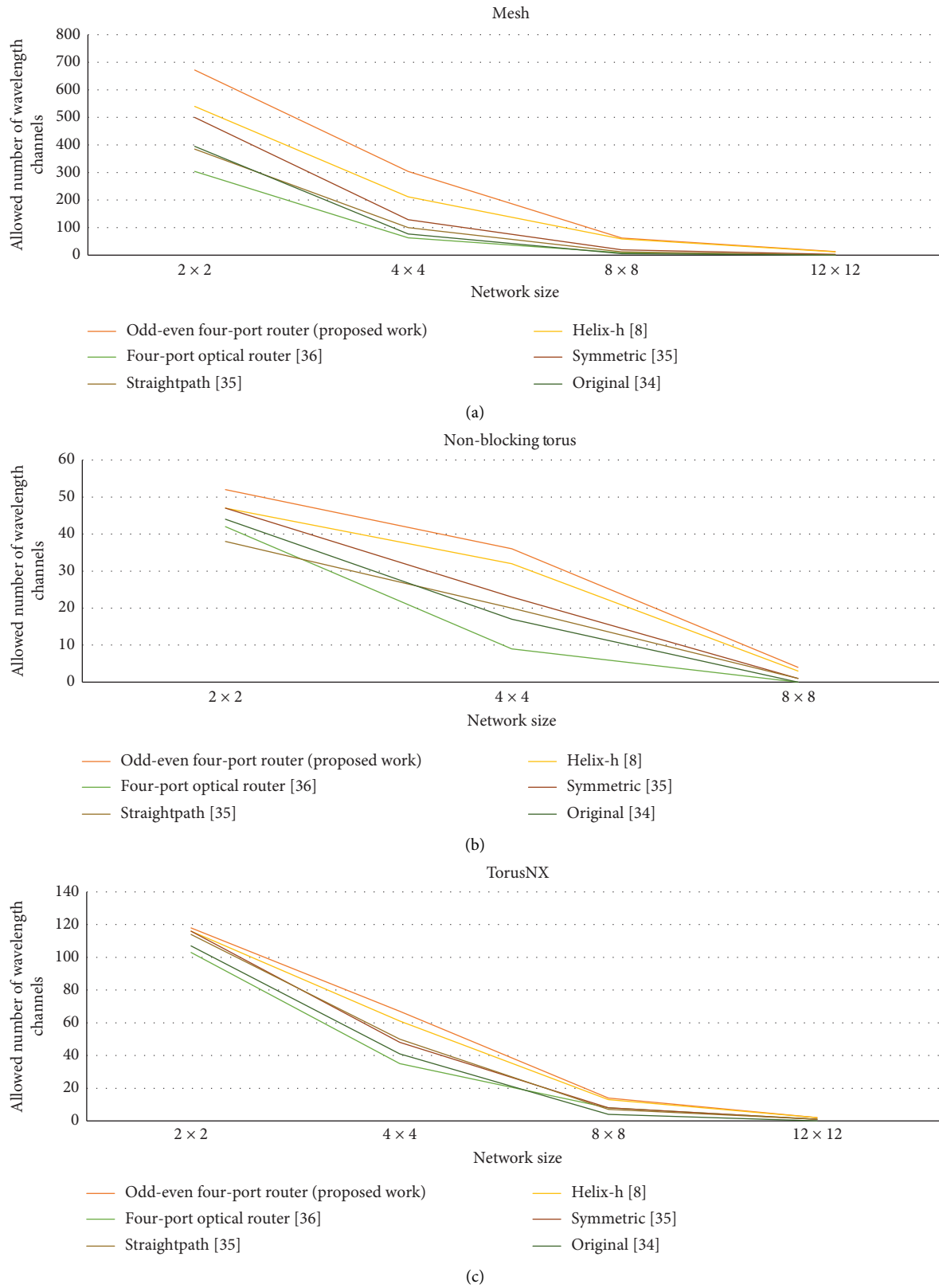


FIGURE 14: Permissible wavelength channels for different network sizes across various routers with a 35-dB optical power budget in (a) Mesh, (b) Nonblocking Torus, and (c) TorusNX topologies.

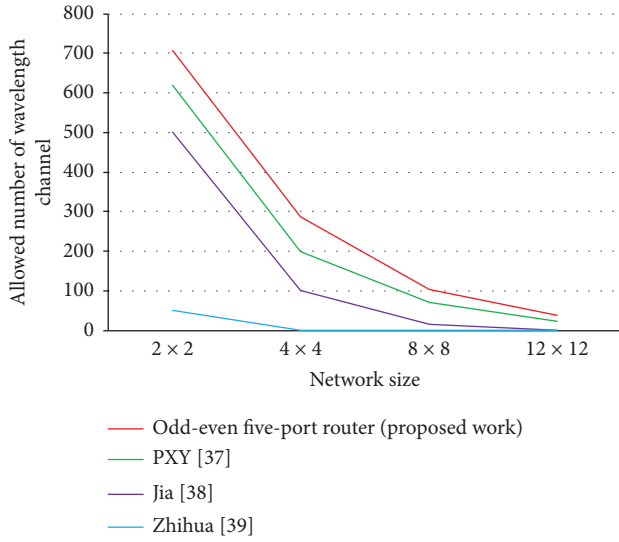


FIGURE 15: Permissible wavelength channels across various routers with a 35-dB optical power budget in mesh topology.

Figure 14 illustrates the diagram depicting the permissible wavelength channels for each of the routers listed in Table 18 during network scaling. Utilizing the Odd-Even four-port router in Mesh, Nonblocking Torus, and TorusNX topologies significantly improves performance in terms of bandwidth and scalability.

With a 35-dB data, the optical power budget of our proposed Odd-Even five-port router enables the mesh topology to scale up to 196 nodes; in contrast, in 5×5 optical routers [38, 39], the network is limited to expanding to 16 and 64 nodes, respectively. Furthermore, within a 64-node mesh, employing the PXY router [37] and the 5×5 optical router [38], only 72 and 9 wavelength channels are available, whereas our proposed Odd-Even five-port router supports 105 wavelength channels.

It can be seen that utilizing MRR-based five port, which is designed for the Odd-Even turn model in a mesh topology, provides performance improvements in terms of bandwidth density and scalability. Figure 15 illustrates the diagrams of some allowed number of wavelength channels when using all the routers as mentioned above (Table 19) in the mesh as the network grows.

4.2.5. Examining the Results of the Proposed MRR-Based Odd-Even Scalable Router Design. Analyzing the proposed MRR-based Odd-Even scalable optical router was led to present general formulas for calculating the number of MRRs, waveguide crossings, and waveguide bending proposed router per N input/output ports. The most indispensable item in the network IL is primarily determined by the quantity of switching components incorporated in the design of optical routers, which directly affects the maximum number of wavelength channels that can be used for simultaneous transmission of optical data and improvement of the network performance. Table 21 shows the results of comparing the proposed design with previous scalable

TABLE 21: The number of switching elements in MRR Odd-Even $N \times N$ scalable optical routers.

| Optical router | The number of MRR |
|-----------------------------------|-------------------|
| Proposed Odd-Even scalable router | $2(N - 2)$ |
| Scalable router [41] | $N(N - 2)$ |
| Scalable router [42] | $N \log_2 N$ |

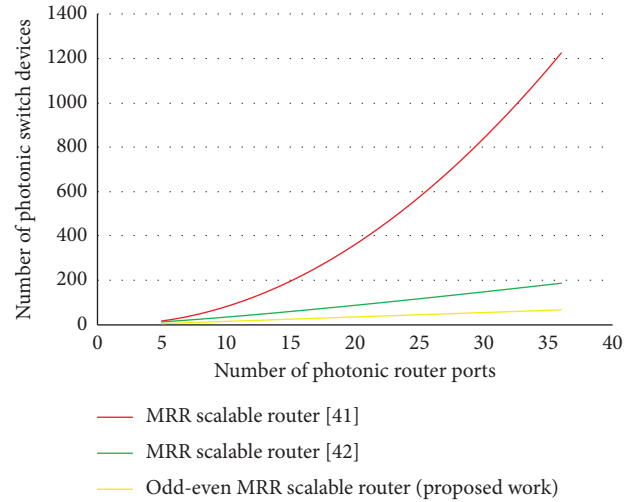


FIGURE 16: The growth of the number of MRR because of an increase in the number of I/O ports.

MRR-based designs regarding the count of switching elements implemented within the architecture of an optical router design per N I/O ports.

As shown in Figure 16, the rate of increase in the switching elements of the proposed scalable router is lower than that of the other designs examined. This is attributed to the design of the proposed five-port Odd-Even router, where inputs are arranged on one side and outputs on the other, forming the core of the scalable router architecture. Furthermore, when an I/O port is added, only a single photonic switch is added from each side. As a result, the number of photonic devices in the proposed scalable Odd-Even router increases gradually yet linearly in comparison to the other configurations. Reducing the number of switching elements effectively lowers the IL, thereby enhancing the performance of the PNoC. Additionally, the proposed design is a scalable, deadlock-free router, whereas the other routers are designed in a more general manner. Consequently, the proposed design is a more appropriate choice for implementation in PNoC. The results confirm the practical benefits and improved performance of the proposed Odd-Even scalable optical router designs for PNoC.

5. Conclusion

In this work, we developed and introduced 4×4 , 5×5 , and scalable optical routers based on the Odd-Even routing scheme within ONoCs. By minimizing the use of MZIs, MRRs, waveguide crossings, and bending structures, the proposed designs achieve a notable reduction in IL while

simultaneously improving the efficiency of wavelength channel utilization. Consequently, these improvements lead to enhanced bandwidth density and greater scalability. The routers are particularly suitable for high-throughput optical interconnects and deliver faster data transmission compared with previously reported optical router architectures employing MRRs and MZIs. To validate their routing capability, the Odd–Even MZI- and MRR-based optical routers were simulated using OptiSystem and PhoenixSim platforms, where a 20-Gbps optical signal was transmitted through each selected port across 10 and 18 available physical paths.

In this study, the key performance indicators for ONoC design were the maximum achievable Q-factor and the minimum BER. Analysis of the Odd–Even four- and five-port as well as scalable optical routers demonstrates that these designs deliver a substantial enhancement in overall network performance.

Data Availability Statement

The data used to support the findings of this study are available from the corresponding author upon reasonable request.

Conflicts of Interest

The authors declare no conflicts of interest.

Funding

The authors declare that no specific funding was received for this work.

References

- [1] U. U. Nisa and J. Bashir, "Towards Efficient on-Chip Communication: A Survey on Silicon Nanophotonics and Optical Networks-on-Chip," *Journal of Systems Architecture* (2024).
- [2] Y. Asadi, "Optical Network-on-Chip (onoc) Architectures: A Detailed Analysis of Optical Router Designs," *Journal of Semiconductors* 46, no. 3 (2025): 031401, <https://doi.org/10.1088/1674-4926/24060006>.
- [3] M. Fadhel, L. Huang, and H. Gu, "RRW: A Reliable Ring Waveguide-Based Optical Router for Photonic Network-on-Chips," in *Parallel Architectures, Algorithms and Programming. Paap 2021. Communications in Computer and Information Science*, ed. L. Ning, V. Chau, and F. Lau, 1362 (Singapore: Springer, 2021), 429–438, https://doi.org/10.1007/978-981-16-0010-4_37.
- [4] M. R. Yahya, N. Wu, F. Zhou, G. Yan, F. Ge, and Z.-U. Abidin, "SMOR: Design of an Optimized 5×5 Nonblocking Optical Router for Photonic Nocs Constructed via Silicon Microring Optical Switch," *Optical Engineering* 59, no. 04 (April 2020): 1, <https://doi.org/10.1117/1.OE.59.4.046104>.
- [5] N. Bagheri Renani and E. Yaghoubi, "A Review of Optical Routers in Photonic Networks-on-Chip: A Literature Survey," *Journal of Advances in Computer Engineering and Technology* 4, no. 3 (2018): 143–154.
- [6] N. B. Renani, E. Yaghoubi, N. Sadehnezhad, and T. Abbasi, "NLR-OP: A High-Performance Optical Router Based on North-Last Turning Model for Multicore Processors," *The Journal of Supercomputing* 78, no. 2 (2021): 2442–2476, <https://doi.org/10.1007/s11227-021-03920-3>.
- [7] J. Chan, G. Hendry, A. Biberman, and K. Bergman, "Architectural Exploration of Chip-Scale Photonic Interconnection Network Designs Using Physical-Layer Analysis," *Journal of Lightwave Technology* 28, no. 9 (2010): 1305–1315, <https://doi.org/10.1109/jlt.2010.2044231>.
- [8] H. Shabani, A. Roohi, A. Reza, M. Reshadi, N. Bagherzadeh, and R. F. Demara, "Loss-Aware Switch Design and Non-Blocking Detection Algorithm for Intra-Chip Scale Photonic Interconnection Networks," *Ieee Transactions on Computers* 65, no. 6 (2016): 1789–1801, <https://doi.org/10.1109/tc.2015.2458866>.
- [9] M. Seifolahi and E. Yaghoubi, "Non-Blocking Routers Design Based on West First Routing Algorithm & MZI Switches for Photonic Noc," *Journal of Advances in Computer Research* 10 (2019): 59–72.
- [10] T. Zhou, H. Jia, and J. Dai, "Rearrangeable-Nonblocking Five-Port Silicon Optical Switch for 2-D-Mesh Network on Chip," *Ieee Photonics Journal* 10, no. 3 (2018): 1–8, <https://doi.org/10.1109/jphot.2018.2841401>.
- [11] S. Zhao, L. Lu, L. Zhou, D. Li, Z. Guo, and J. Chen, " 16×16 Silicon Mach-Zehnder Interferometer Switch Actuated With Waveguide Microheaters," *Photonics Research* 4, no. 5 (2016): 202–207, <https://doi.org/10.1364/prj.4.000202>.
- [12] N. Dupuis, B. G. Lee, A. V. Rylakov, et al., "Design and Fabrication of low-Insertion-Loss and Low-Crosstalk Broadband 2×2 Mach-Zehnder Silicon Photonic Switches," *Journal of Lightwave Technology* 33, no. 17 (2015): 3597–3606, <https://doi.org/10.1109/jlt.2015.2446463>.
- [13] S. Vahidifar and M. Reshadi, "Loss-Aware Routing Algorithm for Photonic Networks on Chip," *The Journal of Supercomputing* 73, no. 12 (2017): 5496–5514, <https://doi.org/10.1007/s11227-017-2096-5>.
- [14] G.-M. Chiu, "The odd-Even Turn Model for Adaptive Routing," *IEEE Transactions on Parallel and Distributed Systems* 11, no. 7 (2000): 729–738, <https://doi.org/10.1109/71.877831>.
- [15] A. Shacham, K. Bergman, and L. P. Carloni, "Photonic Networks-on-Chip for Future Generations of Chip Multiprocessors," *Ieee Transactions on Computers* 57, no. 9 (2008): 1246–1260, <https://doi.org/10.1109/tc.2008.78>.
- [16] H. Wang, M. Petraccia, A. Biberman, B. G. Lee, L. P. Carloni, and K. Bergman, "Nanophotonic Optical Interconnection Network Architecture for on-Chip and off-Chip Communications," in *Optical Fiber Communication Conference* (2008), Jtha92.
- [17] J. Chan, G. Hendry, K. Bergman, and L. P. Carloni, "Physical-Layer Modeling and System-Level Design of Chip-Scale Photonic Interconnection Networks," *Ieee Transactions on Computer-Aided Design of Integrated Circuits and Systems* 30, no. 10 (2011): 1507–1520, <https://doi.org/10.1109/tcad.2011.2157157>.
- [18] G. Du, D. Liang, Y. Song, and D. Zhang, "A Dynamic and Mixed Routing Algorithm for 2D Mesh Noc," in *2013 International Conference on Anti-Counterfeiting, Security and Identification (ASID)* (2013), 1–4, <https://doi.org/10.1109/ICASID.2013.6825285>.
- [19] J. K. Singh, A. K. Swain, T. N. Kamal Reddy, and K. K. Mahapatra, "Performance Evaluation of Different Routing Algorithms in Network on Chip," in *2013 IEEE Asia Pacific Conference on Postgraduate Research in Microelectronics and Electronics (PrimeAsia)* (2013), 180–185, <https://doi.org/10.1109/PrimeAsia.2013.6731201>.

- [20] L. Lyu, L. Song, C. Gao, et al., "Calibration-Free Silicon Photonic Non-Blocking 6×6 Mach-Zehnder Switch," *Journal of Lightwave Technology* 42, no. 7 (2024): 2422–2428, <https://opg.optica.org/jlt/abstract.cfm?URI=jlt-42-7-2422>, <https://doi.org/10.1109/jlt.2023.3337321>.
- [21] P. Bahrebar and D. Stroobandt, "The Hamiltonian-Based odd-even Turn Model for Maximally Adaptive Routing in 2D Mesh Networks-on-Chip," *Computers & Electrical Engineering* 45 (2015): 386–401, <https://doi.org/10.1016/j.compeleceng.2014.12.009>.
- [22] N. Dahir, T. Mak, R. Al-Dujaili, and A. Yakovlev, "Highly Adaptive and Deadlock-Free Routing for Three-Dimensional Networks-on-Chip," *IET Computers & Digital Techniques* 7, no. 6 (2013): 255–263, <https://doi.org/10.1049/iet-Cdt.2013.0029>.
- [23] T. Zhou, H. Jia, J. Ding, L. Zhang, X. Fu, and L. Yang, "on-Chip Broadband Silicon Thermo-Optic 2×2 Four-Mode Optical Switch for Optical Space and Local Mode Switching," *Optics Express* 26, no. 7 (2018): 8375–8384, <https://doi.org/10.1364/oe.26.008375>.
- [24] J. Chan, G. Hendry, A. Biberman, K. Bergman, and L. P. Carloni, "Phoenixsim: A Simulator for Physical-Layer Analysis of Chip-Scale Photonic Interconnection Networks," in *2010 Design, Automation & Test in Europe Conference & Exhibition (DATE 2010)* (2010), 691–696, <https://doi.org/10.1109/date.2010.5457114>.
- [25] D. Yan, H.S. Cao, Y. Yang, and Q. Yang, "Intelligent Network Security Chip Based on Risc-V: A Next Generation Secure Processing Solution," *Seventh International Conference on Advanced Electronic Materials, Computers, and Software Engineering (AEMCSE 2024)* (2024): 114, <https://doi.org/10.1117/12.3038704>.
- [26] A. Varga, "Discrete Event Simulation System," in *Proceedings of the European Simulation Multiconference (ESM'2001)* (2001), 1–7.
- [27] W. Bogaerts, P. Dumon, D. V. Thourhout, and R. Baets, "Low-Loss, low-Cross-Talk Crossings for Silicon-on-Insulator Nanophotonic Waveguides," *Optics Letters* 32, no. 19 (2007): 2801–2803, <https://doi.org/10.1364/ol.32.002801>.
- [28] F. Xia, L. Sekaric, and Y. Vlasov, "Ultracompact Optical Buffers on a Silicon Chip," *Nature Photonics* 1, no. 1 (2007): 65–71, <https://doi.org/10.1038/nphoton.2006.42>.
- [29] L. Liang, K. Zhang, and C. T. Zheng, " $N \times N$ Reconfigurable Nonblocking Polymer/silica Hybrid Planar Optical Switch Matrix Based on Total-Internal-Reflection Effect," *Ieee Photonics Journal* 9, no. 4 (2017): 1–11, <https://doi.org/10.1109/jphot.2017.2718019>.
- [30] M. Geng, Z. Tang, K. Chang, X. Huang, and J. Zheng, "N-Port Strictly Non-Blocking Optical Router Based on Mach-Zehnder Optical Switch for Photonic Networks-on-Chip," *Optics Communications* 383 (2017): 472–477, <https://doi.org/10.1016/j.optcom.2016.09.023>.
- [31] K. Liu, L. Wang, C. Zhang, Q. Ma, and B. Qi, "Compact InGaAsP/InP Nonblocking 4×4 Trench-Coupler-Based Mach-Zehnder Photonic Switch Fabric," *Applied Optics* 57, no. 14 (2018): 3838–3846, <https://doi.org/10.1364/ao.57.003838>.
- [32] E. Yaghoubi, M. Reshadi, and M. Hosseinzadeh, "Mach-Zehnder-Based Optical Router Design for Photonic Networks on Chip," *Optical Engineering* 54, no. 3 (2015): 035102, <https://doi.org/10.1117/1.oe.54.3.035102>.
- [33] S. G. Johnson, C. Manolatos, S. Fan, P. R. Villeneuve, J. D. Joannopoulos, and H. A. Haus, "Elimination of Cross Talk in Waveguide Intersections," *Optics Letters* 23, no. 23 (1998): 1855–1857, <https://doi.org/10.1364/ol.23.001855>.
- [34] A. Shacham, B. G. Lee, A. Biberman, K. Bergman, and L. P. Carloni, "Photonic Noc for DMA Communications in Chip Multiprocessors," in *15th Annual Ieee Symposium on High-Performance Interconnects (HOTI 2007)* (2007), 29–38.
- [35] J. Chan, A. Biberman, B. G. Lee, and K. Bergman, "Insertion Loss Analysis in a Photonic Interconnection Network for on-Chip and off-Chip Communications," in *Leos 2008-21st Annual Meeting of the Ieee Lasers and Electro-Optics Society* (2008), 300–301, <https://doi.org/10.1109/leos.2008.4688609>.
- [36] C. Li, W. Zheng, P. Dang, C. Zheng, Y. Wang, and D. Zhang, "Silicon-Microring-Based Thermo-Optic Non-Blocking Four-Port Optical Router for Optical Networks-on-Chip," *Optical and Quantum Electronics* 48, no. 12 (2016): 552–22, <https://doi.org/10.1007/s11082-016-0825-2>.
- [37] H. Shabani, A. Roohi, A. Reza, H. Khademolhosseini, and M. Reshadi, "Parallel-XY: A Novel Loss-Aware Non-Blocking Photonic Router for Silicon Nano-Photonic Networks-on-Chip," *Journal of Computational and Theoretical Nanoscience* 10, no. 6 (2013): 1510–1514, <https://doi.org/10.1166/jctn.2013.2881>.
- [38] H. Jia, Y. Zhao, L. Zhang, et al., "Five-Port Optical Router Based on Silicon Microring Optical Switches for Photonic Networks-on-Chip," *Ieee Photonics Technology Letters* 28, no. 9 (2016): 947–950.
- [39] Z. Yu, Q. Zhang, X. Jin, J. Zhao, H. Baghsiahi, and D. R. Selviah, "Microring Resonator-Based Optical Router for Photonic Networks-on-Chip," *Quantum Electronics* 46, no. 7 (2016): 655–660, <https://doi.org/10.1070/qel15964>.
- [40] B. G. Lee, A. Biberman, P. Dong, M. Lipson, and K. Bergman, "All-Optical Comb Switch for Multiwavelength Message Routing in Silicon Photonic Networks," *Ieee Photonics Technology Letters* 20, no. 10 (2008): 767–769, <https://doi.org/10.1109/lpt.2008.921100>.
- [41] R. Min, R. Ji, Q. Chen, L. Zhang, and L. Yang, "A Universal Method for Constructing N-Port Nonblocking Optical Router for Photonic Networks-on-Chip," *Journal of Lightwave Technology* 30, no. 23 (2012): 3736–3741, <https://doi.org/10.1109/jlt.2012.2227945>.
- [42] Z. Wang, J. Xu, P. Yang, Z. Wang, L. H. K. Duong, and X. Chen, "High-Radix Nonblocking Integrated Optical Switching Fabric for Data Center," *Journal of Lightwave Technology* 35, no. 19 (2017): 4268–4281, <https://doi.org/10.1109/jlt.2017.2737659>.